

UC San Diego

UC San Diego Electronic Theses and Dissertations

Title

Investigating the Contribution of the Amino- and Carboxy-Terminus of G alpha Protein Families for Receptor Specificity and Efficient Downstream Signaling

Permalink

<https://escholarship.org/uc/item/7b51j47b>

Author

Walters, Geneva

Publication Date

2021

Peer reviewed|Thesis/dissertation

UNIVERSITY OF CALIFORNIA SAN DIEGO

Investigating the Contribution of the Amino- and Carboxy-Terminus of G alpha Protein Families
for Receptor Specificity and Efficient Downstream Signaling

A thesis submitted in partial satisfaction of the requirements
for the degree Master of Science

in

Biology

by

Geneva Lea Ann Walters

Committee in charge:

Professor Roger Sunahara, Chair
Professor Elizabeth Villa, Co-Chair
Professor Barry Grant

2021

The thesis of Geneva Lea Ann Walters is approved, and it is acceptable in quality and form for publication on microfilm and electronically.

University of California San Diego

2021

III

“The universe is full of magical things patiently waiting for our wits to grow sharper.”

~ Eden Phillpotts

TABLE OF CONTENTS

Thesis Approval Page	iii
Epigraph	iv
Table of Contents	v
List of Abbreviations	vii
List of Figures	viii
List of Tables	ix
Abstract of Thesis	x
Introduction	1
1.1 GPCRs and Heterotrimeric G Protein Signaling	1
1.2 G Proteins	3
1.2.1 The Gs Family and Disease	3
1.2.2 The Gi Family and Disease	4
1.2.3 The Gq Family and Disease	5
1.3 G α Subunit Structure, Function, and Chaperones	6
1.3.1 Structure and Function	6
1.3.2 Chaperone Ric-8B	9
1.4 On GPCR-G Protein Selectivity	10
1.4.1 Selective and Promiscuous Coupling	10
1.4.2 Structure Dictating Selectivity	11
1.4.2.1 Carboxy-terminus Investigations	11
1.4.2.2 Amino-terminus Investigations	13
1.5 Recent Discoveries	15

1.5.1 Time-Resolved Mass Spectroscopy Techniques	15
1.5.2 Recent Chimeras by Jelinek et al. (2021)	16
1.6 Biosensors and cAMP Measurement	18
1.7 Ligand-Biased Signaling	19
1.7.1 Significance of Salmeterol	19
1.8 Project Aims	20
2. Methods and Materials	22
2.1 Materials	22
2.2 Methods	26
2.2.1 Plasmid Construction	26
2.2.2 Plasmid Preparation and Quantification of DNA	29
2.2.3 Cell Culture and Transfection	31
2.2.4 cAMP Assay of Wild-Type and Chimeric G proteins	32
2.2.5 Data Analysis	33
3. Results	34
4. Discussion	37
5. Conclusions	41
5.1 Future Studies	42
References	44

List of Abbreviations

ADP	Adenosine Disphosphate
AHD	Alpha Helical Domain
AHD	Alpha Helical Domain
AHO	Albright hereditary osteodystrophy
APC	Anticoagulant-Activated Protein C
β_2 AR	Beta-2 Adrenergic Receptor
cAMP	Cyclic adenosine monophosphate
CTX	Cholera Toxin
DAG	Diacylglycerol
ECL	Extracellular Loop
ERK 1/2	Extracellular Signal-Regulated Kinase 1/2
FRET	Fluorescence Resonance Energy Transfer
GDP	Guanosine Diphosphate
GEF	Guanine Nucleotide Exchange Factors
GPCR	G Protein Coupled Receptor
GDP	Guanosine Diphosphate
GTP	Guanosine Triphosphate
HDF-MS	Hydroxyl Radical Mediated Protein Footprinting-Mass Spectrometry
HDX-MS	Hydrogen/Deuterium Exchange-Mass Spectrometry
ICL	Intracellular Loop
IP3	Inositol 1,4,5-triphosphate
M ₃	Muscarinic Acetylcholine Receptor
NAD	Nicotinamide Adenine Dinucleotide
PAR ₁	Protease-Activated Receptor 1
PIP2	Phosphatidylinositol (4,5) Biphosphate
PKA	Protein Kinase A
PKC	Protein Kinase C
PLCb	Phospholipase Cb
PTX	Pertussis Toxin
RHD	Ras-Homology Domain
TM	Transmembrane

LIST OF FIGURES

Figure 1.1: General Structure of G protein coupled receptors (GPCRs)	2
Figure 1.2: Heterotrimeric G protein family signaling	3
Figure 1.3: Ribbon structures of the $G\alpha_s$ subunit and the beta-2 adrenergic receptor (β_2AR) in complex with the entire heterotrimer G_s protein	7
Figure 1.4: Location of guanine nucleotide ($GTP\gamma S$) coordination on the $G\alpha_s$ subunit and important contact sites between β_2AR and $G\alpha_s$ in nucleotide free conditions	9
Figure 1.5: Amino- and carboxy-termini of $G\alpha_i$ and $G\alpha_o$ are necessary for carbachol-stimulated M_2AChR G protein activation	15
Figure 2.1: “NBC” naming scheme for chimeric $G\alpha$ subunit constructs	27
Figure 2.2: Overview of swapped regions from wild type $G\alpha$ subunits	27
Figure 2.3: PCR thermocycle	28
Figure 3.1: Analysis of wild type $G\alpha_s$ protein induced cAMP accumulation using the Pink Flamindo cAMP biosensor in DGNAS cells	34
Figure 3.2: Analysis of $G\alpha_s$ -based chimera induced cAMP accumulation using the Pink Flamindo cAMP biosensor in DGNAS cells	35

LIST OF TABLES

Table 2.1: List of Primers.....	22
Table 2.2: PCR Reaction Mixture Components.....	23
Table 2.3: PCR Cycling Parameters.....	24
Table 2.4: Stocks, Buffers, Reagents and Chemicals.....	24
Table 2.5: List of Antibiotics and Toxins.....	26
Table 2.6: Summary of EC ₅₀ Values.....	37

ABSTRACT OF THESIS

Investigating the Contribution of the Amino- and Carboxy-Terminus of G Protein Families for Receptor Specificity and Efficient Downstream Signaling

by

Geneva Lea Ann Walters

Master of Science in Biology

University of California San Diego, 2021

Professor Roger Sunahara, Chair
Professor Elizabeth Villa, Co-Chair

G Protein-Coupled Receptors (GPCRs) represent one of the largest and physiologically relevant families of cell surface receptors which mediate extracellular signals through the direct and selective interaction with heterotrimeric G proteins. GPCRs have also been observed coupling to multiple G protein families, yet the structural drivers of this type of selectivity, or

promiscuity, haven't been fully explored. Current models in the field suggest that selectivity by the GPCR is primarily driven by the carboxy-terminal end of the $G\alpha$ subunit of the heterotrimeric G protein complex, but more recent studies have identified other important regions to explore i.e., the $G\alpha$ amino terminus. To address this, we generated a library of chimeric $G\alpha_s$ subunits through site-directed mutagenesis in which the carboxy-termini and/or amino-termini from different families were swapped and replaced to explore each motif's influence on the GPCR-G protein interaction. The activity of the chimeras were indirectly measured using a FRET-based assay to detect the downstream second messenger cAMP using HEK293 cells in which endogenous $G\alpha_s$ subunits have been disrupted. While the results of the data collected show a synergistic effect when both regions are replaced, an extended literature review has inarguably revealed the amino-terminus to be among a group of important structural players influencing selectivity of GPCRs, along with the $\alpha N/\beta 1$ hinge, the $\beta 2/\beta 3$ loop, and the carboxy-terminus, which all have varying influences depending on the receptor. Overall, the findings herein provide important insights into the selectivity determinants related to the GPCR-G protein selection process and identify motifs outside of the carboxy-termini.

Introduction

1.1 GPCRs and Heterotrimeric G Protein Signaling

In the plasma membrane of all eukaryotic cells lies the most studied and largest family of receptors called, G Protein-Coupled Receptors (GPCRs)^{1,2,3}. This family of receptors is the target of roughly 35% of all FDA approved drugs⁵¹, such as the beta-2 adrenergic receptor (β_2 AR) partial agonist salmeterol which is a popular treatment of bronchospasm in patients with moderate to severe asthma¹⁶. GPCRs are the third largest family of genes in the human genome, as more than 800 genes are included in this family¹⁰. Additionally, GPCRs can be categorized into six different classes that are based on their sequence similarities and their functions: Class A, Class B, Class C, Class D, Class E, Class F¹⁷. Class A (rhodopsin-like receptors) can be further categorized into two subtypes: rhodopsin GPCRs and non-rhodopsin GPCRs (such as the β_2 AR)¹⁷. Based on the significant role Class A receptors play in mammalian physiology and how widely they are studied regarding their therapeutic relevance in cancer, asthma, and cardiovascular disease research, they are of particular interest in this study.

Structurally, Class A GPCRs, such as the β_2 AR, share a specific set of characteristics that lend to their common structures (Figure 1.1a and 1.1b). More specifically, all have a relatively short amino-terminus (N-term), followed by a seven-transmembrane α -helical region (TM1-TM7). The TMs are linked by three extracellular loops (ECL1-3) and three intracellular loops (ICL1-3)¹⁷. On the extracellular side, the amino-terminal end of the GPCR and the ECLs bind to various physiologically important extracellular stimuli, such as hormones, neurotransmitters, or even light and assist in the transduction of these signals within the cell¹⁰. When activated by one of these stimuli, GPCRs undergo conformational changes leading to recruitment and activation of one of the four families of heterotrimeric guanine nucleotide-binding proteins on the opposite

side of the plasma membrane (G proteins: Gs, Gi/o, Gq/11, or G12/13). Heterotrimeric G proteins are composed of a guanine-nucleotide binding G α -subunit and an obligate dimer containing the G β and G γ subunits. G $\alpha\beta\gamma$ heterotrimers are held on the plasma membrane via lipid anchors on the G α and G γ subunits ¹¹.

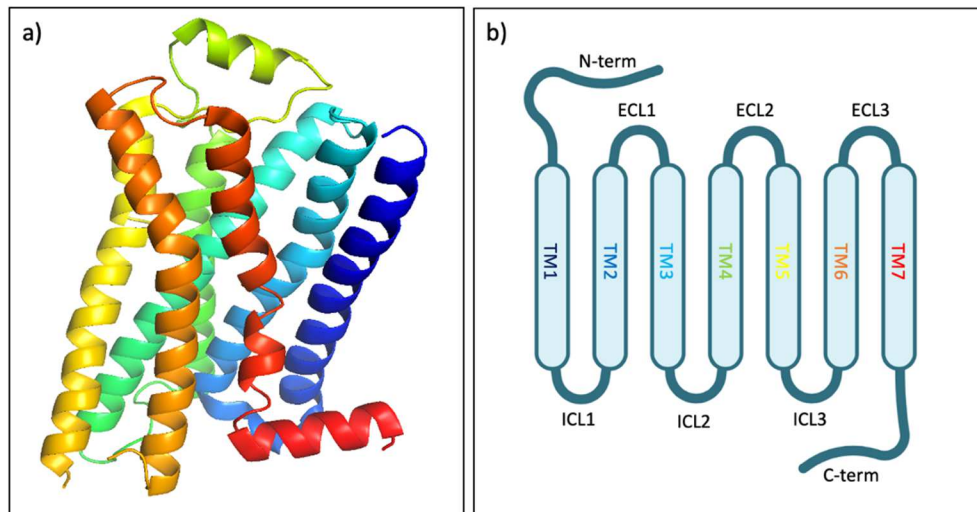


Figure 1.1: General Structure of G protein coupled receptors (GPCRs). (a) The ribbon structure of the beta-2 adrenergic receptor (β_2 AR) where each helix is colored uniquely (PDB: 3PDS). The agonist, FAUC50, and the T4L fusion protein used to stabilize the crystal structure have been omitted for clarity. Visualized in PyMol. (b) Schematic representation of a general GPCR structure showing the amino-terminus (N-term), transmembrane helices 1-7 (TM1-7), intracellular loops 1-3 (ICL1-3), extracellular loops 1-3 (ECL1-3), and the carboxy-terminus (C-term). Created with BioRender.com.

Classically, the GPCR-G protein signaling cascade occurs through a multistep process initially through coupling, promotion of nucleotide exchange, heterotrimer dissociation, GTP hydrolysis on the G α subunit, and the ultimate reassociation of the G $\alpha\beta\gamma$ heterotrimer. First, G proteins are thought to couple to activated GPCRs through a direct interaction between the G α -subunits carboxy-terminus (C-term) and the intra-cellular facing core of the receptor ^{11,17}. Here it is currently thought that engagements with the activated GPCR results in conformational changes within the G α subunit allowing guanosine diphosphate molecule (GDP) dissociation and subsequent exchange for a guanosine triphosphate molecule (GTP) ¹¹. GTP binding to the G α

subunit results in a further conformational change resulting in a functional dissociation from the $G\beta\gamma$ dimer, which allows both $G\alpha$ and $G\beta\gamma$ to separately regulate downstream effector proteins and initiate cell type-specific responses (Figure 1.2)¹². The hydrolysis of GTP to GDP by the $G\alpha$ subunit intrinsic GTPase activity signals the termination of the signaling cascade through promoting reassociation with $G\beta\gamma$ and formation of the inactive heterotrimer¹¹. We will limit the scope and detail of this paper to $G\alpha_s$, $G\alpha_{i/o}$, and $G\alpha_{q/11}$ -dependent signaling.

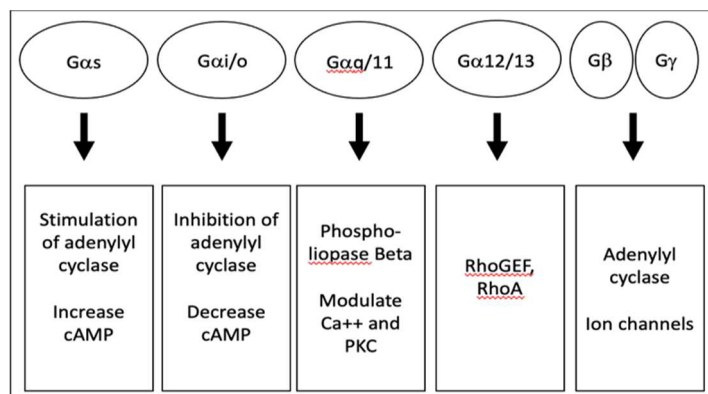


Figure 1.2: Heterotrimeric G protein family signaling. $G\alpha$ subunit subtypes ($G\alpha_s$, $G\alpha_{i/o}$, $G\alpha_{q/11}$, and $G\alpha_{12/13}$) are activated by G protein coupled receptors (GPCRs) in response to ligand binding. After the functional dissociation of $G\alpha$ from $G\beta\gamma$, the activated G protein subunits separately transduce signals to specific effectors.

1.2 G Proteins

1.2.1 The Gs Family and Disease

The first heterotrimeric G protein to be discovered was the stimulatory G protein, G_s ¹⁹. There are two G_s subtypes, $G\alpha_s$ and $G\alpha_{olf}$, where $G\alpha_s$ displays a ubiquitous expression pattern while $G\alpha_{olf}$ is predominantly expressed in the olfactory system¹⁹. There are two major and one minor splice forms of $G\alpha_s$ subunit, $G\alpha_{s(short)}$, $G\alpha_{s(long)}$ and $G\alpha_{s(XL)}$, respectively. $G\alpha_{s(short)}$, $G\alpha_{s(long)}$ are generally co-expressed at similar levels within a single cell type within nearly all mammalian cell systems¹⁹. Additionally, all $G\alpha_s$ subunits are susceptible to modifications made by cholera toxin (CTX), which is an enterotoxin made by *Vibrio cholerae*²¹. More specifically,

Arg201, located in the alpha helical domain (AHD) of $G\alpha_s$, is adenosine diphosphate (ADP)-ribosylated by the toxin¹⁹. This arginine residue is conserved in all $G\alpha$ subunits and contributes toward GTPase reaction (e.g. conversion of GTP back to GDP) and is thus critical for G protein inactivation¹⁹. Mutations of Arg201, or ADP-ribosylation by cholera toxin, thus inactivates the subunits intrinsic GTPase activity and causes $G\alpha_s$ to be constitutively active¹⁹. Prolonged $G\alpha_s$ activation leads to prolonged protein kinase A (PKA)-mediated signaling causing catastrophic symptoms of cholera poisoning (e.g. diarrhea and dehydration), or in the case of Arg²⁰¹ mutations, can cause cancer and several diseases¹⁹.

In contrast to mutations that cause constitutively active forms of $G\alpha_s$, heterozygous inactivating $G\alpha_s$ mutations have been found to cause Albright hereditary osteodystrophy (AHO)⁴¹. The heterozygous mutations have been found to cause a decrease (~50%) in functional $G\alpha_s$ present/expressed in erythrocytes and other tissues collected from patients⁴¹. While the loss-of-function disorder has been known to manifest in many ways, it is mainly characterized by short stature, short bones in hands and feet, subcutaneous ossification, obesity, and occasionally, developmental delays⁴¹. Diseases such as this signal the importance of G proteins and their physiological relevance within the cell.

1.2.2 The Gi Family and Disease

In opposition to the $G\alpha_s$ subunit, the majority members of $G\alpha_i$ subunits work to decrease cAMP levels when necessary while some of the members of the $G\alpha_i$ family are potent regulators of voltage-gated cation channels, most notably voltage-dependent K^+ and Ca^{2+} channels³⁹. There are eight genes encoding the $G\alpha_i$ family members: $G\alpha_{i1}$, $G\alpha_{i2}$, $G\alpha_{i3}$, $G\alpha_o$, $G\alpha_z$, $G\alpha_{t1}$, $G\alpha_{t2}$ and gustducin ($G\alpha_{t3}$). Each $G\alpha_i$ family member, except $G\alpha_z$, is uniquely sensitive to pertussis toxin

(PTX) secreted by *Bordetella pertussis*¹⁹. PTX, like cholera toxin, uses nicotinamide adenine dinucleotide (NAD) as a substrate to ADP-ribosylate the carboxy-terminus of the $G\alpha_i$ subunit¹⁹. More specifically, the modification occurs four amino acids in from the C-terminal end at a conserved cysteine residue located four residues in from the C-terminal end¹⁹. ADP ribosylation of this Cys disrupts interactions with the GPCR intracellular core, effectively preventing coupling of the G_i heterotrimer to the receptor, which locks the $G\alpha_i$ subunit in an inactive, GDP-bound state²⁴. Ribosylated $G\alpha_i$ is therefore no longer capable of inhibiting adenylyl cyclase, allowing unregulated accumulation of cAMP, overexpression of cAMP- and PKA-inducible genes that regulate proliferation, differentiation, and survival of numerous cell-types which leads to multiple clinical pathologies²⁴.

1.2.3 The Gq/11 Family and Disease

Although $G\alpha_q$ and $G\alpha_{11}$ are encoded by distinct genes, the proteins share the same number of amino acids, are located on the same chromosome, and are functionally indistinguishable⁴⁰. Unlike G_s or G_i , activation of members of the Gq family by a Gq/11-coupled receptor, like the M1 muscarinic acetylcholine receptor (M_1AChR), leads primarily to activation of phospholipase C β (PLC β). The PLC β isoform leads to two separate second messengers, inositol 1,4,5-triphosphate (IP₃) and diacylglycerol (DAG) from the substrate phosphatidylinositol (4,5) biphosphate (PIP₂)⁴⁰. While DAG is a potent activator of protein kinase C (PKC) isoforms, IP₃ activates IP₃-gated calcium channels (ryanodine receptor) on the endoplasmic reticulum (sarcoplasmic reticulum in muscle cells) and causes release of calcium into the cytoplasm (promotes contraction in muscle cells)⁴⁰.

Interestingly, aberrations in $G\alpha_q$ signaling has been linked to multiple conditions in genetically modified mouse studies. Efficient $G\alpha_q$ activation by Gq coupled receptors plays a role in the development of heart failure⁴⁰. In mouse models, cardiomyopathies and heart failure occurs from overexpression of $G\alpha_q$ or constitutively activated $G\alpha_q$ ⁵². Transgenic models in mice expressing an inducible $G\alpha_q$ genetically engineered to prevent interaction with PLC β failed to produce similar pathologies suggesting that over-activation of PLC β is related to heart failure⁵². Additionally, another study done in $G\alpha_q$ -deficient mice showed that bleeding time and resistance to thromboembolism was increased substantially compared to wild-type animals, suggesting that $G\alpha_q$ plays an important role in platelet aggregation⁴⁰. Therefore, a better understanding of the Gq/11 family and their relationships with GPCRs at a structural level could lend to better therapeutics.

1.3 $G\alpha$ Subunit Structure, Function, and Chaperones

1.3.1 Structure and Function

There are 17 genes corresponding to 21 different $G\alpha$ subunits sharing 40% overall conserved amino acids, while also sharing 60-90% identity within subtypes^{19,23}. These $G\alpha$ isoforms can be broken up into four distinct families, primarily based on the downstream effectors which they regulate. In terms of structure and function, each $G\alpha$ subtype shares a common architecture and molecular mechanism. Multiple crystal structures of different $G\alpha$ -subunits have revealed that the guanine nucleotide binding pocket is contained in a compact domain that is structurally like the small family of G proteins in the ras family³³. This region is referred to as the ras-homology domain (RHD). What distinguishes heterotrimeric G proteins from the ras family of G proteins is an extra domain within $G\alpha$, the alpha helical domain (AHD),

named after its high content of alpha-helical structure (Figure 1.3) ¹¹. Guanine nucleotide binding is primarily contributed by residues in the RHD but is influenced by tight interactions with the AHD ¹¹. Like many nucleotide-lyases, e.g. ATPases and GTPases, diphosphate and triphosphate forms are heavily coordinated within the G α subunit by residues within the phosphate binding loop (P-loop), the so-called GAGES box (Gly-Ala-Gly-Glu-Ser) ³⁰, but also by residues within the β_5 - α_4 and β_6 - α_5 loops on the RHD ¹¹.

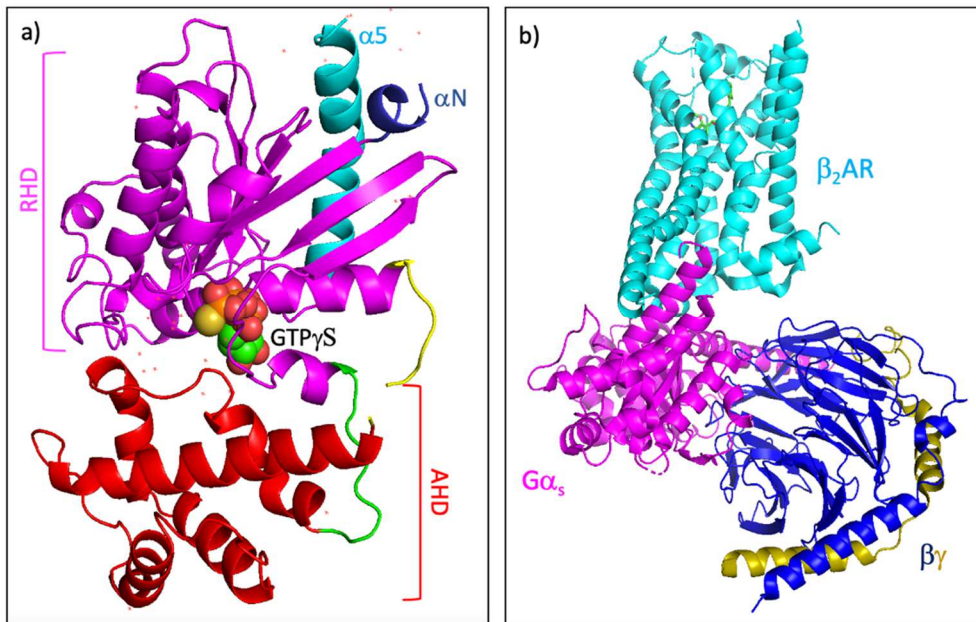


Figure 1.3: Ribbon structures of the G α_s subunit and the beta-2 adrenergic receptor (β_2 AR) in complex with the entire heterotrimer Gs protein. Visualized using PyMol. **(a)** Structure of the G α_s subunit complexed with guanosine 5'-O-(3-thiotriphosphate) (GTP γ S) shown as spheres (PDB: 1AZT). The structure is color coded as follows: magenta is the ras-homology domain (RHD), red is the alpha-helical domain (AHD), cyan is the α_5 helix (C-terminus), blue is part of the α_N helix (N-terminus), yellow is linker 1, and green is linker 2. **(b)** Structure an agonist-bound, nucleotide-free β_2 AR (cyan) complexed with the Gs protein heterotrimer (G α_s subunit: magenta, G β subunit: blue, G γ subunit: yellow). The camelid antibody fragment and T4 lysozyme used to stabilize the crystal structure have been omitted for clarity (PDB: 3SN6).

Interestingly, the points of contact on the G α subunit where the guanine nucleotide is coordinated is linked to important GPCR-G protein regions of interaction. For example, the outward movement of TM6 of an activated GPCR (facilitated by ligand binding) opens enough for the carboxy-terminus (α_5 helix) of G α to insert into the intracellular core of the receptor ²⁰.

Additionally, the P-loop which coordinates the second or beta phosphate (β -[PO₄]) of GDP or GTP, is linked to the G α 's N-terminus by the highly conserved β_1 strand (Figure 1.4). This P-loop is a highly conserved region that is found in G α subunits of heterotrimeric G proteins as well as small molecular weight G proteins, such as the ras family⁵⁷. Consequently, it appears that disordering the P-loop and disrupting coordination of the β -[PO₄] of GDP, thus allowing its release, is considered a critical step that occurs prior to G protein activation through GTP binding in both types of G proteins³¹. Important to note, the site of interaction of the G α N-term, which leads into the β_1 - α_1 loop (P-loop), is primarily within the second intracellular loop (ICL2) of the GPCR¹¹. ICL2 is located directly after the highly conserved DRY motif of GPCRs, located in the third transmembrane domain¹⁷. In almost all receptor-G protein structures, ICL2 of the receptor adopts a short helical conformation and interacts directly with the G α N-term⁵³. Mutations in ICL2 have been shown to exhibit strong phenotypes on G protein activation, implying that this region is involved in G protein coupling¹¹. Thus, at least from a structural perspective, it seems reasonable that involvement of the G α N-terminus and its proximity to the β_1 -strand in P loop, should be important in nucleotide exchange across all G protein families. The fact that strong interactions between the N-termini of G α and GPCR have been seen in almost all GPCR-G protein complex structures⁵⁴, in addition to the C-termini, this suggests that perhaps a coordinated contribution of both termini are required for efficient coupling and downstream signaling. While this relationship is suspected, further research still needs to be done.

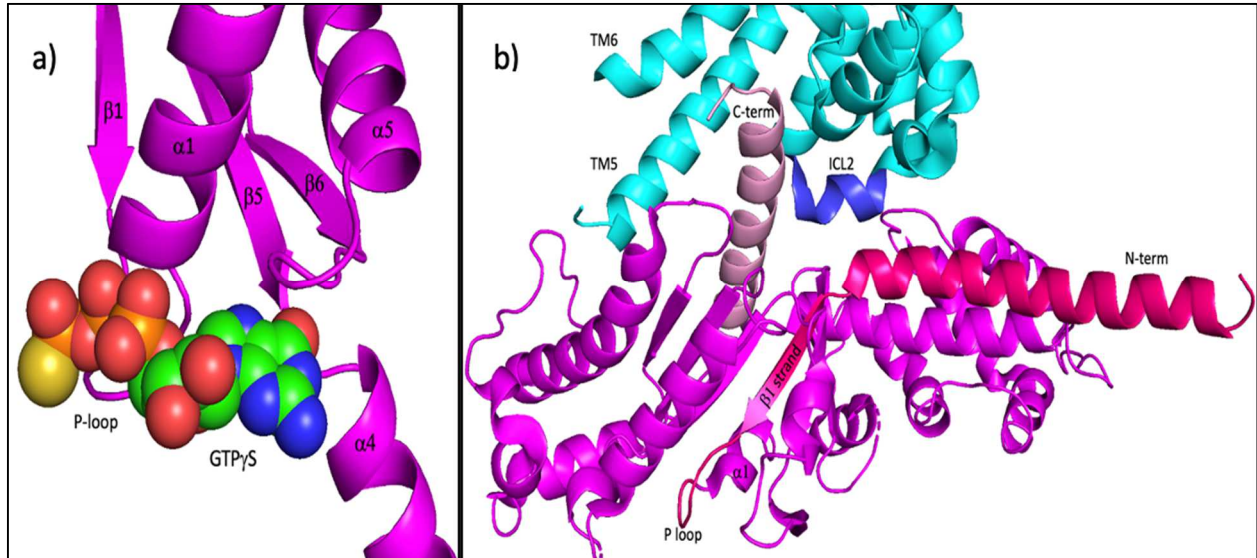


Figure 1.4: Location of guanine nucleotide (GTP γ S) coordination on the G α_s subunit and important contact sites between β_2 AR and G α_s in nucleotide free conditions. Visualized using PyMol. **(a)** Close up cartoon structure of the β_1 - α_1 loop (P-loop), β_6 - α_5 loop, β_5 - α_4 loop interacting with the phosphates and purine ring of GTP γ S (represented as spheres). (PDB: 1AZT). **(b)** β_2 AR (blues)-G α_s (pinks) complex showing the carboxy-terminus (C-term) extended into the intracellular core of the receptor and the interaction between ICL2 of the receptor with the amino-terminus (N-term)- β_1 hinge which leads into the β_1 - α_1 loop (P-loop) where the guanine nucleotide phosphates are coordinated. (PDB: 3SN6).

1.3.2 Chaperone Ric-8B

Ric-8 proteins (~60 kDa) act as molecular chaperones that positively regulate the α subunit of heterotrimeric G proteins⁴². There are two distinct genes responsible for making Ric-8A and Ric-8B that are present in mammals, frogs, and fish⁴³. In mammals, while Ric-8A prefers binding to G $\alpha_{i/o}$, G $\alpha_{q/11}$, G $\alpha_{12/13}$ subunits, Ric-8B exclusively prefers G $\alpha_{s/olf}$ subunits⁴³. One study found that newly translated G α subunits were prone to rapid degradation in the absence of Ric-8 in the cell (using Ric-8A or Ric-8B knock out embryonic stem cell lines), supporting the chaperone role and protection against the α subunit unfolding after translation, prior to membrane association⁴³. Additionally, it has been suggested that Ric-8 proteins can act as non-GPCR guanine nucleotide exchange factors (GEFs)⁴³. Ric-8B overexpression was shown to enhance coupling efficiency of odorant receptors when G α_{olf} and G $\beta\gamma$ were also

overexpressed⁴², although this observation may be the result of improved $G\alpha_{olf}$ stability rather than contributions to GEF activity. Taken together, these studies suggest the potential importance of co-overexpression of cognate Ric-8 in G protein overexpression assays, which is relevant to this current study.

1.4 On GPCR-G Protein Selectivity

1.4.1 Selective and Promiscuous Coupling

Efficient and selective coupling between a GPCR and a specific G protein family is crucial for initiating essential cellular signaling cascades¹². For example, epinephrine binds to the β_2 AR, which classically promotes the stimulatory heterotrimeric G protein (Gs) to couple to the receptor¹². After nucleotide exchange on the $G\alpha$ subunit ($G\alpha_s$) and the functional dissociation of $G\alpha_s$ from $G\beta\gamma$ occurs, the $G\alpha_s$ subunit goes on to directly stimulate adenylyl cyclase to make the second messenger cyclic adenosine monophosphate (cAMP) which activates protein kinase A (PKA), which phosphorylates and changes the activity of many important players involved in metabolism¹³. Conversely, the cAMP response can also be modulated by β_2 AR recruitment of the inhibitory heterotrimeric G protein (Gi), which inhibits adenylyl cyclase and thus decreases intracellular cAMP when necessary¹³. Interestingly, structural analysis of the β_2 AR-Gi complex reveals that ICL2 of the receptor does not adopt an alpha helical structure, which is in contrast to the β_2 AR-Gs complex³⁴. This suggests that the interaction between ICL2 and the N-terminus of the $G\alpha$ subunit could be important for efficient coupling between cognate receptor-G protein pairs. While β_2 AR has a preference to couple to Gs over Gi³⁴, the nature of this selectivity or promiscuity, which is physiologically relevant, is still poorly understood across all GPCR-G protein relationships.

In fact, it has been found that GPCRs are capable of coupling to any one of the four major G protein families. GPCR promiscuity suggests that distinct regions within the G α subunits amino acid sequence act as selectivity determinants for their cognate receptors more so than others ⁷. From an evolutionary perspective based on inferences from sequence alignments, Flock et al. (2017) suggests that because there are G α subtype-specific residues surrounding universally conserved GPCR-G protein interface positions, selective binding by certain GPCRs is ensured, yet promiscuous binding is still achieved. They went on to compare the relationship between GPCRs and G proteins to a lock and key mechanism, where the G protein is the lock and GPCRs are keys with non-identical cuts ⁷. To extend this analogy, considering the amino- and carboxy-termini are part of the subtype specific residue regions observed interacting with receptors ¹¹, replacement of one or both regions should lead to receptor coupling and recognition dictated by the swapped termini regions. While this study theoretically predicts regions (protein-protein recognition sites) that are important outside of the suspected G α C-terminus based on sequence alignments and structures ⁷, there is still a need to uncover more molecular details through experimentation.

1.4.2 Structure Dictating Selectivity

1.4.2.1 C-terminus investigations

Over the years, it has been strongly suggested that the C-term of the G α subunit is the most important selectivity determinant. Especially considering the crystal structures showed with overwhelming evidence that the C-terminal helix of G α subunit fits snugly into the intracellular cavity of the receptor, which suggests this region is particularly important in the receptor-G protein interaction ³⁵. This has placed a significant amount of focus to be put on the G α subunit's

C-term in the GPCR field. For example, Sandhu *et al.* (2019) used C-terminal peptides of $G\alpha_s$, $G\alpha_i$, and $G\alpha_q$ protein subunits to show that each adopts a unique orientation when coupled to their cognate GPCR. Unfortunately, because the study only focused on the C-term of the $G\alpha$ subunits, their conclusions underestimate the importance of the entire G protein heterotrimer for efficient coupling and signaling e.g., $G\beta\gamma$ plays a major role in positioning the N-term of $G\alpha$ so that it can interact with ICL2 on the receptor¹¹. In another example, the crystal structure of the adenosine A_{2A} receptor ($A_{2A}R$) bound to an engineered “mini-Gs” protein exhibited many features and interaction sites like the β_2AR -Gs crystal structure^{31,44}. The study showed 14 residues from the C-term of the mini-Gs protein packing against TM3, ICL2, TM5, TM6, TM7 and TM8 of $A_{2A}R$, similar to the β_2AR -Gs structure. While these findings seem to signal the importance of the C-term across receptor-G protein interactions, the study underestimated the importance of additional sites of interaction of native G proteins. In fact, the mini-Gs protein, in addition to lacking an AHD, the engineered $G\alpha$ was missing 25 amino acids from the extreme N-terminus, regions which, as mentioned earlier, interact with $G\beta\gamma$ and ICL2 of the receptor. Thus, while these studies have helped to uncover and solidify important details regarding GPCR-G protein interactions and contact sites, these peptides or mini- $G\alpha_s$ studies do not encapsulate the entire temporal sequence of the GPCR-G protein dynamic that leads to efficient signaling and don't reveal an obvious selectivity ‘barcode’.

Another methodology to investigate the importance of structural motifs relies on chimeric proteins. Indeed, engineered chimeras of G proteins where the C-termini between two $G\alpha$ isoforms were swapped have been successfully evaluated. For example, by replacing the C-term of $G\alpha_q$ with $G\alpha_i$, classic $G\alpha_i$ -coupled receptors (e.g., dopamine D2 and adenosine A_1 receptors) lead to the activation of phospholipase C, which is normally coupled to $G\alpha_q$ receptors⁴⁶.

Interestingly, $G\alpha_q$ chimeras containing only five C-terminal residues from $G\alpha_s$ were capable of allowing the $G\alpha_s$ -coupled vasopressin V2 receptor to regulate phospholipase C⁴⁷, suggesting that as little as the last five residues of the C-term appear to be critical for receptor-G protein specificity. Thus, C-terminal chimeras between $G\alpha$ isoforms have been examined and are generally in good agreement and support the role of the C-term in receptor-G protein specificity.

However, a largely underappreciated property of these receptor-chimeric $G\alpha$ interactions is that the coupling efficiency is underestimated. Dose-response, the concentration of agonist required to fully activate the effector is typically much higher than coupling to the receptor's cognate or native G protein. Additionally, it has been found that splice variants of $G\alpha_o$ couple to different receptors even though their last 8 amino acids (C-termini) are identical⁴⁷. Thus, although the C-terminus does contribute toward receptor coupling, there must be other regions of the G protein that play a role in coupling specificity and efficiency.

1.4.2.2 N-terminus investigations

Essentially, the field has put a significant focus on the sole contribution of the $G\alpha$ C-term and have overshadowed the contributions of the N-term, a region supported by biochemical and structural data¹¹. However, a series of studies previously performed by the Johnson laboratory pin-pointed a series of residues in the N-terminus of $G\alpha_s$ and $G\alpha_i$ critical to both G protein activation (GDP dissociation) and for receptor specificity^{58, 59}. As mentioned previously, structural data on various GPCR-G protein complexes have implicated the $G\alpha$ N-term and ILC2 of the receptor as critical for receptor catalyzed nucleotide exchange. Not only that, in the case of initial protein recognition and selective receptor binding, the role of the N-term has been suspected, but not thoroughly investigated. N-terminal truncations of $G\alpha_t$ (transducin) reveal that

the N-term is critical for rhodopsin-catalyzed nucleotide exchange⁵⁵. Additionally, similar studies involving chimeric CB₁/CB₂ cannabinoid receptors identified ICL2 of the CB₁ receptor to be responsible for mediating G_s and G_i specific coupling⁶⁰. Strikingly, truncations up to the highly conserved KLLLL sequence (β 1-strand) were incapable of being activated by light-stimulated rhodopsin, despite being able to form a receptor-G protein complex⁵⁵. Another truncation study reported that deletion of a unique 6 amino acid extension present on the N-terminus of the G α_q subunit permits coupling to several different G_i- and G_s-coupled receptors productively interacted with the truncated protein⁴⁸. This suggests that, at least in the case of G_q-coupled receptors, the N-terminus is important for constraining the receptor to bind selectively to G_q and potentially alludes to an important role the N-terminus plays in the initial receptor-G protein interaction but still doesn't fully address the role it plays in efficient G protein activation. Preliminary biochemical data from the Sunahara Lab suggest that the G α protein's amino-terminal end greatly contributes to GPCR-G coupling selectivity and protein recognition to achieve efficient downstream signaling (Figure 1.5, unpublished, 2021). As illustrated in Figure 1.5a, when the C-term of G α_s is replaced with that of G α_i (N_s•G α_s •C_i, red), the dose-response curve related to carbachol stimulation of M₂AChR is right shifted when compared to native, wild type G α_i (blue) coupling. Interestingly, the additional replacement of the N-term with that of G α_i (N_i•G α_s •C_i, magenta) resulted in the restoration of the dose-response relationship of carbachol with sensitivities similar to native G α_i (blue) coupling. Therefore, there is a growing appreciation from structural and biochemical data of GPCR-G protein complexes that efficient and specific coupling involves engagement of both the N- and C-terminal ends of G α subunits with the receptor¹¹. For these reasons we rationalized that replacement of both

termini in G protein chimeras should lead to much more efficient receptor coupling and a panel of potentially useful chimera for further GPCR studies.

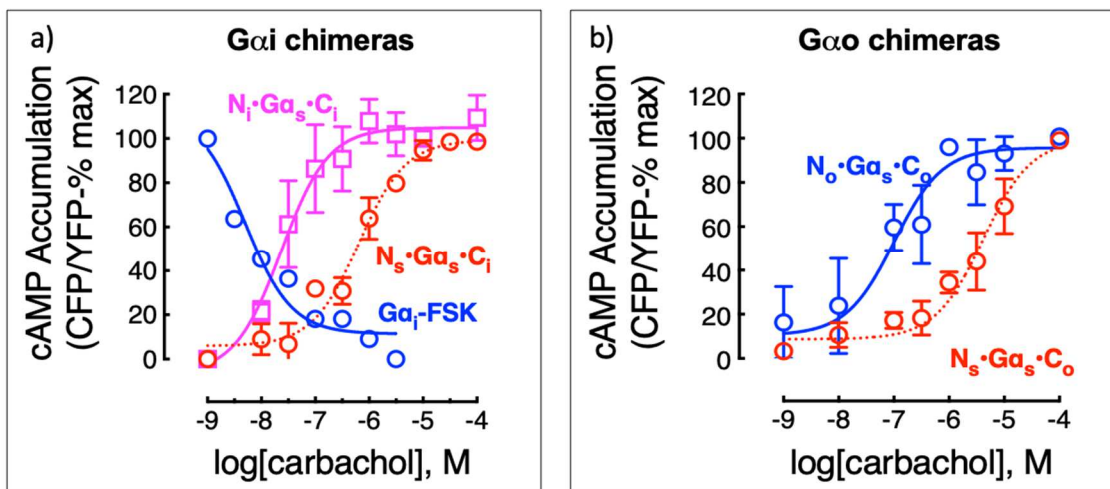


Figure 1.5: Amino- and carboxy-termini of $G\alpha_i$ and $G\alpha_o$ are necessary for carbachol-stimulated M_2 AChR G protein activation. cAMP accumulation is represented as percentage normalized to the maximum agonist-induced response individual to each chimeric $G\alpha_s$ -based protein (CFP/YFP-%max). Using Δ GNAS cells, $G\alpha_i$ - $G\alpha_s$ (a) and $G\alpha_o$ - $G\alpha_s$ (b) chimeras with termini regions systematically swapped, similar to the chimeras generated in this current study, were co-transfected with the M_2 AChR and a dose-response curve to carbachol was performed (Vasquez and Sunahara, unpublished). For comparison purposes, the carbachol dose response curves for M_2 AChR-mediated inhibition of forskolin-stimulated adenylyl cyclase through coupling to $G\alpha_i$ was included in panel a (blue symbols). Chimeras shown are pertussis insensitive mutants (C352G). Error bars represent \pm SEM.

1.5 Recent Discoveries

1.5.1 Time-Resolved Mass Spectroscopy Techniques

Successful x-ray crystal structures of GPCR-G protein complexes have revolutionized the field and helped uncover important interaction sites within the complex. While structural studies provide important snapshots into GPCR-G protein complexes, the inanimate nature of the structures and nucleotide-free state in which they are stabilized fail to assess the temporal sequence of the coupling events. Recently, time-resolved techniques, such as hydrogen/deuterium exchange mass spectrometry (HDX-MS) and hydroxyl radical-mediated

protein footprinting with mass spectrometry (HRF-MS), have been helpful tools for revealing structural changes that happen during the sequence of coupling events in the hopes of figuring out a general GPCR-G protein coupling mechanism³⁵. Considering that unraveling the coupling mechanism could explain the selective and specific nature of class A GPCRs, a recent study using both techniques mentioned suggests that the G α C-term is necessary for efficient engagement but that N-terminal interaction with the receptor ICL2 of the receptor is critical for GDP release³⁵. Furthermore, the authors suggest that the structures of the nucleotide-free β_2 AR-Gs complex are conformationally different from the initial transient interaction. While they were not able to determine the exact initial engagement contacts, the initial transient state could represent a selectivity filter. Considering there has been a growing desire to uncover a general mechanism that dictates GPCR-G protein selectivity, this study brings the scientific community one step closer.

1.5.2 Recent Chimeras by Jelinek et al.

In good agreement with our preliminary data, Jelinek et al. (2021) recently characterized the contributions of regions outside of the G α C-term that contribute toward selective coupling and recognition by GPCRs⁴⁹. Here, the authors exchanged N- and C-termini of G α_o and G α_q corresponding to suggested contact sites with GPCRs from previous studies and characterized the binding stabilities, dissociation kinetics, and activation potencies of the two wild-type G proteins (Go and Gq) and analogous sets of G α subunit chimeras (with the same regions swapped from either protein). The authors measured coupling of two Gq-coupled receptors (M₃ and H₁ receptors) in single permeabilized HEK293T cells using a Fluorescence Resonance Energy Transfer (FRET)-based system. Exchanging the last 11 C-terminal amino acids of G α_q

with that of $G\alpha_o$ (GqoC11) impaired the binding stability of the chimera- H_1 receptor complex was noticeably impaired while the same was not true for the M_3 receptor. Moreover, although they found that the binding stability of GqoC11 with the M_3 receptor was only slightly impaired, the activation of the chimera was substantially comprised. Similarly, when the N-terminus from $G\alpha_q$ was replaced with that of $G\alpha_o$ (GqoN), the chimera did not bind to the H_1 receptor at all whereas the chimera could bind to the M_3 receptor but failed to be activated. Additionally, the results showed that the $G\alpha_o$ -based double chimeras (with $G\alpha_o$ as the backbone along with C- and N-termini replaced with $G\alpha_q$) coupled to both receptors with a synergistic effect that was comparable to wild-type Gq results, gaining almost Gq-like properties. In contrast, the opposite construct ($G\alpha_q$ -based double chimeras with the N- and C-termini from $G\alpha_o$) encountered selectivity barriers upon activation by the M_3 receptor, not at complex formation. Lastly, when the β_2/β_3 loop is considered based on its proximity to ICL2 (observed in the M_1 AChR-G11 complex; PDB: 6oij), the authors found that when this region was swapped from $G\alpha_o$ with that of $G\alpha_q$, there was an increase in activation potency and binding stabilities with both of the tested receptors. These findings suggest that selectivity mechanisms are specific to each receptor and potentially occur multiple times during the coupling process. In summary, it appears that the N-terminus (including the α_N/β_1 hinge), the β_2/β_3 loop, and all 22 amino acids from the α_5 helix majorly contribute to coupling specificity. This is remarkable because their data reveals several suspected structures outside of the C-terminus of the $G\alpha$ subunit (such as the N-terminus which is particularly relevant to our current study) that influence selective binding and coupling to the M_3 and H_1 receptors.

1.6 Biosensors and cAMP Measurement

Considering that GPCR-mediated activation of Gs produces a predictable signaling cascade in which the GTP-bound G α subunit directly stimulates adenylyl cyclase to produce cAMP (and inorganic pyrophosphate), an indirect way of studying GPCR-mediated Gs activation involves the measurement of intracellular cAMP²². Several methods of detection have been developed and improved over the last few years, the majority of which are end-point assays using radio-immunoassays to detect cAMP. More recently, real-time intracellular cAMP detection has been made possible and more efficient by the utilization of fluorescent biosensors²². FRET-based biosensors have become particularly useful because they use non-radiative energy transfer between fluorophores in close proximity as a method of detection³⁶. The sensors take advantage of the conformational change that occurs to the sensor upon cAMP binding, therefore, the optimal change in FRET is dependent on the distance and positioning of the fluorescent protein(s) to each other²². One such FRET-based biosensor, the red cAMP indicator called “Pink Flamindo” (Pink Fluorescent cAMP indicator), stands out as being particularly useful in our current study²⁵. The biosensor takes advantage of the cAMP-binding domain of the protein called Epac (Exchange protein directly activated by cAMP 1, residues 205-353) and has it genetically-encoded within the sequence of the red fluorescent protein, mApple (Figure 1.5)²⁵. This allows the fluorescence to be measured at one wavelength instead of two, unlike other FRET-based cAMP indicators using two fluorescent proteins³⁶, and avoids the non-specific activation of adenylyl cyclase caused by blue light since Pink Flamindo utilizes a red-shifted derivative²⁵.

1.7 Ligand-Biased Signaling

A current popular topic in the world of molecular pharmacology is the idea of “ligand-biased signaling”. This is the observation that certain ligands change the conformation of the receptor in a way that promotes the activation and signaling associated with certain G proteins (or other effectors) more so than others ³⁸. For example, protease-activated receptor 1 (PAR₁), which is part of the group A rhodopsin-like GPCRs, is activated by thrombin or trypsin by cleavage at canonical sites, revealing a tethered ligand domain that binds the second extracellular loop on the receptor that induces conformational changes required for downstream signaling ⁴⁵. Interestingly, trypsin or thrombin-activated PAR₁ couple to many different G protein-dependent and independent signaling pathways ⁴⁵. However, because canonical PAR signaling pathways depend on proteases cleaving at specific cleavage sites, proteases that cleave PARs at other locations and reveal unique tethered ligands act to promote non-canonical signaling pathways in a biased manner ⁴⁵. The anticoagulant-activated protein C (APC) cleaves PAR₁ at the canonical site as well as an alternative site, which leads to β -arrestin 2-mediated Rac1 activation which is independent of G protein signaling ⁴⁵. Additionally, APC-activated PAR₁ cannot activate extracellular signal-regulated kinase 1/2 (ERK 1/2) ⁴⁵. Therefore, ligand-biased PAR₁ activation of canonical and non-canonical signaling pathways is dependent on the cleavage site and the specific ligand involved.

1.7.1 Significance of Salmeterol

The partial agonist for β_2 AR, salmeterol, is commonly prescribed for patients with asthma and chronic obstructive pulmonary disease because it acts as a bronchodilator ¹⁸. The popularity surrounding this partial agonist for those conditions are based on two important

properties. Salmeterol has a long duration of action (up to 12 hours) and selectively binds to β_2 AR instead of β_1 AR, which reduces cardiac involvement¹⁸. Our recent crystal structure of salmeterol bound to β_2 AR¹⁸, along with spectroscopic approaches and single molecule studies in support, suggests that salmeterol-bound β_2 AR stabilizes a conformation that is distinct from the epinephrine (full agonist)-bound form of β_2 AR¹⁸. More specifically, while the epinephrine-bound β_2 AR stabilizes a 13 Å outward movement of TM6, salmeterol-bound β_2 AR had an outward movement of only 8 Å¹⁸. Therefore, the difference in movement of TM6 creates a smaller binding pocket in which the C-terminus of the $G\alpha_s$ subunit inserts. Considering that members of the $G\alpha_i$ subfamily have a smaller C-term than $G\alpha_s$, in terms of surface area and volume, coupling of β_2 ARs bound to salmeterol may permit preferential coupling to $G\alpha_i$ over $G\alpha_s$. Our collaborators have recently resolved a structure of a Gi- β_2 AR complex stabilized by salmeterol (unpublished) and the structure appears consistent with this model. Although beyond the capacity of our current study, the N- and C-termini $G\alpha_s/G\alpha_i$ chimeras may be extremely useful for biochemically characterizing salmeterol- vs epinephrine-bound β_2 AR. We are hoping to initiate these studies and use the data as biochemical support for the structural data on the Gi- β_2 AR-salmeterol complex.

1.8 Project Aims

To better understand the potential drivers of GPCR selectivity, the aim of this thesis was to focus on analyzing the current hypotheses through site-directed mutagenesis studies to find the motif(s) that contribute to receptor-G protein interactions in the hopes of deconvoluting some of the promiscuous behavior of G protein-coupled receptors. Obtaining biochemical data that focuses on the N- and C-termini of the $G\alpha$ subunits during receptor-G protein interaction and

coupling efficiency would be extremely useful for understanding receptor-G protein selectivity. Moreover, these studies may unravel adverse reactions of some therapeutics through promiscuous G protein or arrestin coupling, but also potentially reveal strategies for the development of novel biased ligands. To accomplish this goal, we rationally designed chimeric $G\alpha_s$ subunits, mixing and matching both the N- and C-termini from different G protein isoforms and studied coupling efficiency. The designs were based on sequence alignments of all $G\alpha$ subtypes, but also guided by available structural biology data. The chimeras are based on the $G\alpha_s$ subunit core so that we could take advantage of the real-time cAMP sensor Pink Flamindo, as well as a plethora of $G\alpha_s$ -specific reagents available in the Sunahara lab. We limit our study to the β_2 AR and M_3 -acetylcholine receptor (M_3 AChR), which natively couple to G_s , G_i and G_q , respectively. We generated stably expressed Pink Flamindo cAMP biosensor in cells where the genes that dictate the $G\alpha_s$ subtype has been disrupted by a CRISPR/Cas9 system (Δ GNAS) to host transiently transfected $G\alpha$ chimeras of interest. We hypothesized that both the N- and C-termini are equally important for dictating GPCR selectivity and coupling efficiency. The long-term goal is to aid in the discovery of safer and more efficacious therapeutics. We feel that gaining a better understanding of structural basis for receptor-G protein selectivity may aid in developing these safer drugs. In summary, this study focuses on the three representative members of the $G\alpha$ family and aims to determine which motifs within the $G\alpha$ subunit dictate GPCR selectivity, efficient coupling, and G protein activation.

2. Materials and Methods

2.1 Materials

Table 2.1: List of Primers

Primer name	Primer Number	Sequence (5' to 3')	Corresponding construct(s) (NBC naming ⁺)
GNAI into pcDNA 3.1(+) forward	19	CTCACTATAGGGAGACCCAA GATGGGCTGCACGCTGAG	III
GNAI into pcDNA 3.1(+) reverse	20	GGGCCCTCTAGACTCGAGTTAA AA GAGACCACAATCTTTTAGATTAT TTTTTATGATGACATC	III
GNAQ into pcDNA 3.1(+) forward	21	CTCACTATAGGGAGACCCAAGA TGACTCTGGAGTCCATCATGGC	QQQ
GNAQ into pcDNA 3.1(+) reverse	22	GGGCCCTCTAGACTCGAGTTAG ACCAGATTGTACTCCTTCAGGTT C	QQQ
GNAO into pcDNA 3.1(+) forward	23	CTCACTATAGGGAGACCCAAGA TGGGATGTACTCTGAGCGCAG	OOO *
GNAO into pcDNA 3.1(+) reverse	24	GGGCCCTCTAGACTCGAGTCAG TACAAGCCGCAGCCC	OOO *
GNA12 into pcDNA 3.1(+) forward	25	CTCACTATAGGGAGACCCAAGA TGTCCGGGGTGGTGCG	121212 *
GNA12 into pcDNA 3.1(+) reverse	26	GGGCCCTCTAGACTCGAGTCAC TGCAGCATGATGTCCTTCAG	121212 *
GNAS into pcDNA 3.1(+) forward	27	CTCACTATAGGGAGACCCAAGat gggctgtctgggaaacagc	SSS
GNAS + pcDNA 3.1(+) reverse	28	GGGCCCTCTAGACTCGAGTTAga gcagtcatactgacggagg	SSS
I<>SS forward	53	caccagcagcagcagCTTGACCTCGCG CGCC	ISS *
I<>SS reverse	54	GCGCGGAGGTCAAGctgctgctgctg ggtgc	ISS *
SS<>I forward	35	catccagcgcacCTAAAAGATTGT GGTCTCTTTAACTCGAGTCTAG	SSI and ISI
SS<>I reverse	36	CGAGTTAAAAGAGACCACAATC TTTTAGgtgcatgcgctggatgatgc	SSI and ISI
ISI (Pg)** forward	49	TTAAAAGAGACCACCATCTTTTA Ggtgca	ISI (Pg) ***

Table 2.1: Continued

ISI (Pg)** reverse	50	cCTAAAAGATGGTGGTCTCTTTT AACTCGAG	ISI (Pg) ***
Q<>SS forward	46	GACGCCCGCCGGtaccgggccacgcacc	QSS *
Q<>SS reverse	47	GACGCCCGCCGGtaccgggccacgcacc	QSS *
SS<>Q forward	39	catccagcgcacCTGAAGGAGTAC AATCTGGTCTAACTCG	SSQ and QSQ
SS<>Q reverse	40	GTTAGACCAGATTGTACTCCTTC AGgtgcatgcgctggatgatgctc	SSQ and QSQ
O<>SS forward	41	CCGCCAAAGACGTGAAATTAtacc gggccacgcacc	OSS *
O<>SS reverse	48	TAATTTACGTCTTTGGCGGCG	OSS *
SS<>O forward	43	catccagcgcacCTCCGGGGCTGC GGC	SSO and OSO *
SS<>O reverse	44	CGCAGCCCCGGAGgtgcatgcgctggat gatgctc	SSO and OSO *
OSO (Pg) *** forward	51	AAGCCGCCGCCCGG	OSO (Pg) */***
OSO (Pg) *** reverse	52	GGGGCGGCGGCTTGTAC	OSO (Pg) */***
ISI (Pg)** reverse	50	cCTAAAAGATGGTGGTCTCTTTT AACTCGAG	ISI (Pg) ***
Q<>SS forward	46	GACGCCCGCCGGtaccgggccacgcacc	QSS *
Q<>SS reverse	47	GACGCCCGCCGGtaccgggccacgcacc	QSS *

⁺ Refer to Figure 2.1 for description of NBC naming scheme

* These wild-type/chimeric G alpha subunits were made but not utilized in an assay; the genes were transferred into pcDNA3.1(+) from pcDNA3.0(+) for future directions or were an intermediate chimera towards the final construct to be tested in assay.

** “<>” denotes the location at which the different wild-type proteins were joined

*** “Pg” denotes the site-directed mutation from C to G at the fourth residue from the C-terminal end to make the construct insensitive to pertussis toxin.

Table 2.2: PCR Reaction Mixture Components

Components	Concentration	Volume (uL)	Final Concentration	Company
Autoclaved Milli-Q H ₂ O	-	11.5		Millipore, Lab Produced
Q5 Reaction Buffer	5X	5.0	1X	New England BioLabs Inc.
Deoxynucleotide (dNTP) Solution Mix	10 mM	0.5	200 μM	New England BioLabs Inc.
Q5 Hot Start High-Fidelity DNA Polymerase	2,000 units/mL	0.5	0.02 units/μL	New England BioLabs Inc.
DNA template	~1 ng/μL	5	< 1,000 ng	-
Primer pair mixture	variable	2.5	1 μM	Synthesized by Eton Biosciences, La Jolla, CA

Table 2.3: PCR Cycling Parameters

Temperature (°C)	Time (seconds)	Cycles
98	60	X 1
98	20	} X 30
60	30	
72	150-180*	
72	600	X 1
20	∞	

* Variable depending on fragment length

Table 2.4: Stocks, Buffers, Reagents and Chemicals

Buffer/ Reagent/ Stock Solution	Composition/ Company, Catalog No.
Milli-Q Water	Millipore Milli-Q lab water system
6X Gel Loading Dye, Purple	New England Biosciences Inc., Catalog No. B7024S
10X TAE Buffer	48.5 g of Tris base ([tris(hydroxymethyl)aminomethane]) 11.4 mL of glacial acetic acid (17.4 M) 20 mL 0.5 M EDTA (pH 8.0) Deionized water to make 1 L
1X TAE Buffer	50 mL 10X TAE 450 mL Deionized water
1% (w/v) Agarose Gel	0.3 g of agarose powder (Fisher Scientific, Catalog No. BP1356-100) 30 mL 1X TAE 6 µL of a 2.5 mg/mL aqueous solution of ethidium bromide
Quick-Load 1 kb DNA Ladder	New England Biosciences Inc., Catalog No. ND468S
10X CutSmart Buffer	New England Biosciences Inc., Catalog No. B7204S
1X CutSmart Buffer	10 µL 10X CutSmart Buffer 90 µL autoclaved Milli-Q water
PB Buffer	23.88 g guanidine hydrochloride 15 mL isopropanol Autoclaved Milli-Q water to make 50 mL
PE Buffer	50 µL 1M Tris (pH 7.5) 41 mL ethanol Autoclaved Milli-Q water to make 50 mL
5X IT Buffer	1 mL 50% PEG (polyethylene glycol) 8000 in Milli-Q water 0.4 mL 100 mM Tris (pH 7.5) 0.1 mL 50 mM MgCl ₂ 0.1 mL 50 mM DTT (Dithiothreitol) 0.2 mL 1 mM of each dNTPs, New England BioLabs Inc. 0.2 mL 5 mM NAD ⁺ (nicotinamide adenine dinucleotide)

Table 2.4: Continued

Assembly Mixture	200 μ L 5X IT buffer 0.4 μ L T4 Exonuclease, New England BioLabs Inc. 12.4 μ L Phusion DNA Polymerase, NEB Inc. 100 μ L Taq ligase, NEB Inc. 160 μ L 1M Tris (pH 7.5) 277.1 μ L autoclaved Milli-Q water
SOC Media	0.5% (w/v) yeast extract 2% (w/v) tryptone 10 mM NaCl 2.5 mM KCl 10 mM MgCl ₂ 10 mM MgSO ₄ 20 mM glucose Deionized water
LB Media, Liquid	1% (w/v) tryptone 0.5% yeast extract 1% NaCl Deionized water
LB Media, Solid, carbenicillin	500 mL LB media, liquid 7 g agar 500 μ L carbenicillin
Transporter 5	Polysciences, Catalog No. 26008-50
TB (Terrific Broth)	Fisher BioReagents, Catalog No. BP24682
DMEM	Gibco, Catalog No. 12430062
Opti-MEM	Gibco, Catalog No. 11058021
10X PBS	80 g NaCl 2.0 g KCl 14.4 g Na ₂ HPO ₄ 2.4 g KH ₂ PO ₄
1X PBS	50 mL 10x PBS 450 mL deionized water
Lifting Buffer	1X PBS 1.25 mL EDTA (pH 7.2)
1X HBSS (Hank's Balanced Salt Solution)	Corning, Catalog No. 21-023-CM
HEPES (1M) (N-2-hydroxyethylpiperazine-N-2-ethane sulfonic acid)	Gibco, Catalog No. 15630080
HBSS-HEPES	1L 1X HBSS 20 mM HEPES
Isoproterenol	Sigma, Catalog No. I-2760
Carbachol	Sigma, Catalog No. C-4382
Ascorbic Acid	Mallinckrodt, Catalog No. 1852
IBMX (3-isobutyl-1-methylxanthine)	AdipoGen Life Sciences, Catalog No. AG-CR1-3512

Table 2.5: List of Antibiotics and Toxins

Antibiotic/Toxin Name	Stock Concentration	Final Concentration
Zeocin	100 mg/mL	100 μ g/mL
Doxycycline	4 mg/mL	4 μ g/mL
Carbenicillin	100 mg/mL	100 μ g/mL
Pertussis Toxin (PTX)	100 μ g/mL	100 ng/mL

2.2 Methods

2.2.1 Plasmid Construction

cDNAs for human $G\alpha$ subunits were used for the purpose of this study to generate chimeric $G\alpha$ subunits. An open reading frame of three full length, untagged, wild-type $G\alpha$ subunits ($G\alpha_s$, $G\alpha_i$, $G\alpha_q$) were cloned into pcDNA3.1(+) expression plasmid for expression in mammalian cells. Primers were designed that contained sequences encoding the swapped C-termini or N-termini of each wild-type $G\alpha$ subunit. Chimeric $G\alpha$ subunits were created using the synthesized primers (Eton Biosciences). A site-directed mutation was also introduced at the fourth residue from the C-terminal end to the constructs containing the C-terminal sequence of the $G\alpha_i$ subunit to make those constructs insensitive to pertussis toxin ((Pg), C352G). This enabled the measurement of $G\alpha_i$ sequence containing chimera in the absence of endogenous $G\alpha_i$. All primers used, their lengths, and the corresponding chimera it made are listed in Table 2.1 and a schematic representation of the chimeras are shown in Figure 2.1. Refer to Figure 2.2 to see a detailed overview of the chimeras including the specific residues replaced in context of secondary structure as a snake plot.

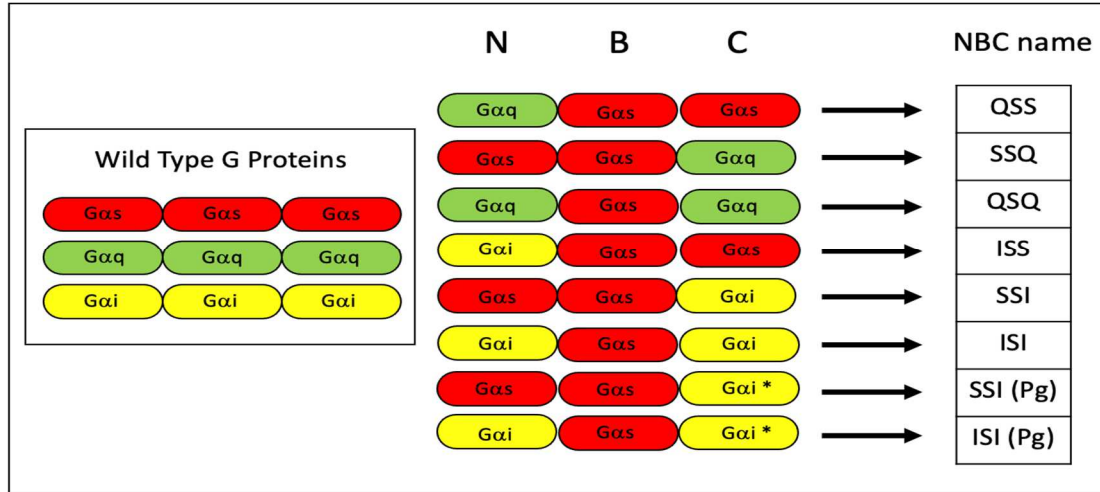


Figure 2.1: “NBC” naming scheme for chimeric Gα subunit constructs. System of naming refers to the three regions of the Gα subunit for context (“N” refers to the amino-terminal end, “B” refers to the base, or core structure, of the subunit, and “C” refers to the carboxy-terminal end). The name generated by this scheme, located to the right of the arrow, contains letters that represent each Gα subunit subtype of origin as a single letter (Gα_s=S, Gα_q=Q, Gα_i=I). Wild type G proteins are color coded and presented on the left as a key. “*” and “(Pg)” indicate a C to G mutation at the 4th C-terminal residue that makes the construct insensitive to pertussis toxin.

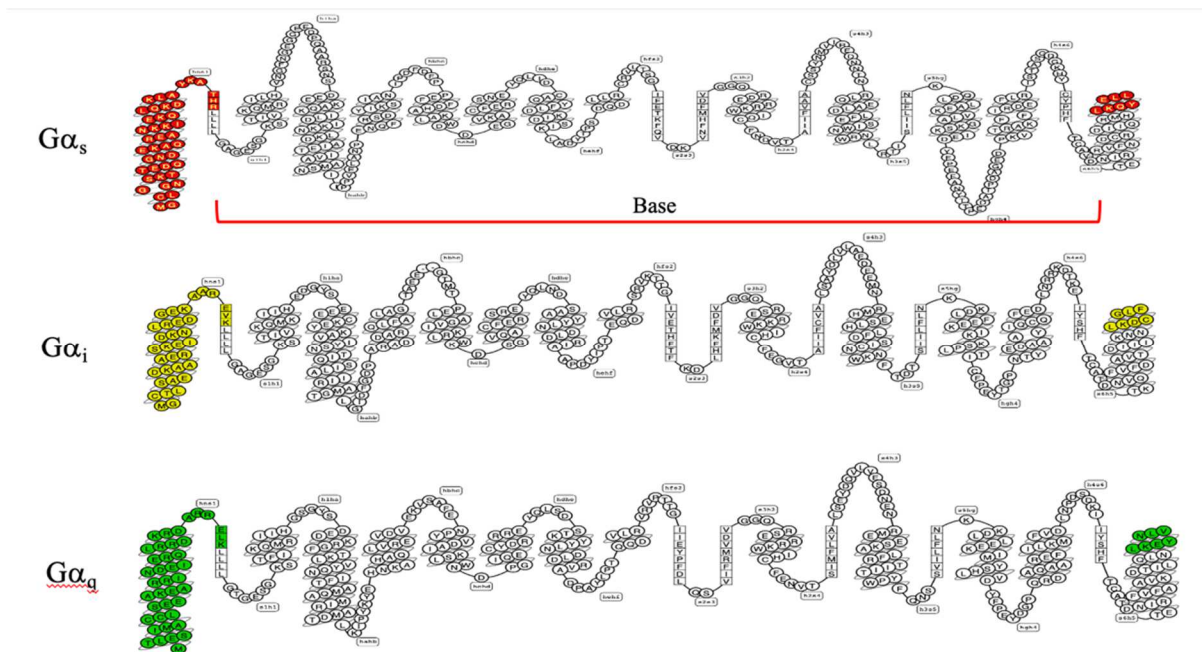


Figure 2.2: Overview of swapped regions from wild-type Gα subunits. Detailed snake plots (obtained from gpcrdb.org) showing specific amino acids that were swapped from each wild-type Gα subunit (Gα_i and Gα_q) onto the base of Gα_s. The yellow (Gα_i) and green (Gα_q) regions were systematically swapped for the red regions. Amino acids are color coded the same as Figure 2.1.

For each forward and reverse primer pair that creates a PCR generated fragment, 1 μL of each was mixed with 38 μL of autoclaved Milli-Q water (primer pair mix). To prepare the PCR reaction mixture, the following components were combined in the follow order for a total of 25 μL and placed in a 96-well, iCycler Thermal Cycler (Bio-Rad) (Refer to Table 2.2): 11.5 μL of autoclaved Milli-Q water (Millipore), 5.0 μL 5X Q5 reaction buffer (New England Biolabs Inc, (NEB)), 0.5 μL dNTP mix (NEB), 0.5 μL Q5 Hot Start High-Fidelity DNA Polymerase (NEB), 5 μL of corresponding dilute DNA template ($\sim 1 \text{ ng}/\mu\text{L}$), and 2.5 μL of the primer pair mix. The PCR cycling parameters were as follows (Table 2.3 and Figure 2.3): initial denaturation step at 98 $^{\circ}\text{C}$ for one minute, followed by 30 cycles of denaturation of template DNA at 98 $^{\circ}\text{C}$ for 20 seconds, annealing at 60 $^{\circ}\text{C}$ for 30 seconds, extension at 72 $^{\circ}\text{C}$ for 2.5-3 minutes (20 seconds per 1000 base pairs), and a final extension step of 72 $^{\circ}\text{C}$ for 10 minutes followed by an infinite hold at 20 $^{\circ}\text{C}$ until ready for use.

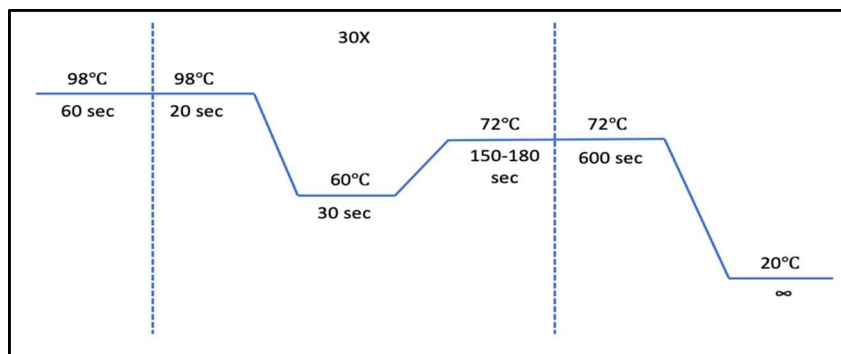


Figure 2.3: PCR thermocycle. Protocol for thermocycle for all PCR reactions performed in a 96-well, iCycler Thermal Cycler (Bio-Rad).

To detect and verify the sizes of each PCR generated DNA fragment, 5 μL of each PCR reaction was mixed with 1 μL of 6X purple loading dye (NEB) and loaded in a pre-cast 1% (w/v) agarose gel containing 6 μL of ethidium bromide (2.5 mg/mL stock concentration) together with a standard marker (Quick-load 1 kb DNA ladder, NEB) (Table 2.4). Electrophoresis was

performed using a Bio-Rad Power/Pac 1000 at 100 volts for 30 minutes through 1X TAE buffer (Table 2.4). The plasmid DNA was visualized using a ChemiDoc™ Touch Imaging System (Bio-Rad) and compared to a reference ladder to determine the number of base pairs.

Prior to fragment purification, 20 µL of each PCR mixture was mixed with 25 µL of 1X CutSmart buffer (NEB) and 0.5 µL of the restriction enzyme *DpnI* (NEB, 20,000 units/mL) and then incubated at 37 °C for 30 minutes. The *DpnI* digested fragments were then purified on a silica-based purification column (UPrep spin column, Genesee Scientific). The fragments were resuspended in 300 µL of buffer PB (Table 2.4) and centrifuged at 7600 RCF (relative centrifugal force) for one minute. After discarding the flow through, the column was washed twice with 700 µL of buffer PE at 7600 RCF (Table 2.4). Autoclaved Milli-Q H₂O (10 µL) was then added to the column and left to incubate at room temperature for two minutes then centrifuged at 7600 RCF for an additional two minutes. The resulting purified fragments were assembled by Gibson Assembly protocol in which 7 µL of Assembly Mix (Table 2.4) was mixed with a 1:1 ratio (1 µL each) of the purified fragments. The mixture was incubated at 50 °C for 15 minutes followed by submersion in a water bath at 37 °C for 30 minutes.

2.2.2 Plasmid Preparation and Quantification of DNA Concentration

Plasmids were transformed into pre-made chemically competent DH5a *E. coli* (*Escherichia coli*) cells by combining 30 µL competent *E. coli* cell stock with the purified fragments mentioned above followed by 20 minutes on ice. The mixture was then heat shocked in a water bath at 42 °C for 60 s followed by another 20 minutes on ice. The mixture was added to a New Brunswick Innova 4000 Incubator Shaker at 220 RPM (rotations per minute) for 30 minutes at 37° C after the addition of 700 µL of SOC media (Table 2.4). The bacterial cells were

then pelleted by centrifugation at 960 RCF for 5 minutes. After the removal of 600 μ L of the supernatant, the remaining 100 μ L was used to resuspend the pellet. The resuspended pellet was then incubated overnight at 37° C in Luria-Bertani (LB) agar media (Table 2.4) containing petri dishes in the presence of carbenicillin (Table 2.5). Colonies were selected by toothpick the next morning and grown in 5 mL of Terrific Broth (TB; Table 2.4) in the presence of carbenicillin (Table 2.5) overnight at 37° C in a shaking incubator (220 rpm, New Brunswick Innova 4000 Incubator Shaker). Bacteria were then harvested by centrifugation at 3480 RCF for 15 min and the supernatant removed.

The plasmids were purified and isolated from the *E.coli* cells using a Thermo Scientific GeneJET Plasmid Miniprep Kit (catalog number: K0502) according to manufacturer's instructions. Additionally, their purifications and concentrations were tested on a NanoDrop™ 2000 Spectrophotometer (Thermo Scientific) using 2 μ L samples, after being zeroed with autoclaved Milli-Q water. Absorbance at 260 nm and 280 nm were measured with a 340 nm correction. All constructs were confirmed by forward and reverse sequencing (Eton Biosciences, La Jolla, CA).

The sequence verified plasmids were then transformed into pre-made chemically competent DH5a *E. coli* cells by combining 15 μ L competent cell stock with 1 μ L of dilute plasmid DNA (~1 ng/ μ L) on ice for two minutes. The mixture was heat shocked in a 42 °C water bath for 60 seconds, followed by an additional two minutes on ice. After the addition of 100 μ L SOC media, the transformation mixture was then incubated overnight at 37° C on LB agar media (Table 2.4) containing petri dishes in the presence of carbenicillin (Table 2.5). Colonies were selected by toothpick the next morning and grown in 50 mL of TB in the presence of carbenicillin overnight at 37° C in a shaking incubator at 220 RPM (New Brunswick Innova

4000 Incubator Shaker). Bacteria were then harvested by centrifugation at 3480 RCF for 15 minutes and the supernatant removed. Finally, a Thermo Scientific GeneJET Plasmid Midiprep Kit (catalog number: K0482) was used to isolate and purify the plasmid DNA at a higher yield. The concentrations were then quantified as mentioned above and the purified plasmids stored at -20 °C until ready for use.

2.2.3 Cell Culture and Transfection

Cloned human embryonic kidney (HEK293) cells, known as Δ GNAS cells, in which genes were knocked out by a CRISPR/Cas9 system corresponding to both members of the $G\alpha_s$ family (genes GNAS and GNAL, encoding $G\alpha_s$ and $G\alpha_{olf}$, respectively), were used in all experiments. These lines were generously provided by Dr. Asuka Inoue (Tohoku University, Japan). Additionally, the Δ GNAS cell line stably expressed a doxycycline inducible Epac sensor (Pink Flamindo) encoded in pcDNA4.0 plasmid and was maintained by the addition of ZeocinTM (10 μ L added per plate at a concentration of 100 mg/mL at the time of seeding). The Δ GNAS cells were cultured in 10 cm tissue culture plates in 10 mL of Dulbecco's Modified Eagle Medium (DMEM, Table 2.4) supplemented with 10% (v/v) heat-inactivated fetal bovine serum (FBS) in an environment of 5% CO₂ at 37° C.

Twenty-four hours prior to and at the time of transfection, 10 μ L of doxycycline (Table 2.5) was added to promote the expression and accumulation of the Pink Flamindo sensor. Additionally at the start of the transfection, the media was replaced by 10 mL of reduced serum media (Opti-MEM, Table 2.4). Transfection was performed using a polyethylenimine (PEI) reagent (Transporter 5, Polysciences). A transfection mixture was prepared in which 600 μ L of reduced serum media, 96 μ L of Transporter 5, 12 μ g of wild-type $G\alpha_s$ or one of the chimeric

plasmids, and 12 µg of the protein chaperone Ric-8B2 were left to incubate for 20 minutes at room temperature and then added dropwise to the cells. For the cases in which a pertussis toxin insensitive chimera was being evaluated or the system was stimulated with carbachol, (ISI (Pg), SSI (Pg), SSQ, QSQ), 10 µL of pertussis toxin (100 µg/mL stock solution) was added to the plates at the time of transfection. Cells were incubated in an environment of 5% CO₂ at 37° C for 24 hours before harvesting and completing the assay described below.

2.2.4 cAMP Assay of wild-type and chimeric G proteins

Twenty-four hours after transfection when the cells reached about 90% confluency, the ΔGNAS cells were harvested by first washing each plate two times with 1X phosphate buffered saline (PBS) (pH 7.4, Table 2.4). The cells were lifted from the plates using 5 mL of a solution of 1X PBS containing 20 mM HEPES (N-2-Hydroxyethylpiperazine-N-2-Ethane Sulfonic Acid) and 1 mM EDTA (pH 7.2) (Lifting Buffer, Table 2.4). The cells were harvested by centrifugation in 15 mL Falcon tubes at 3000 rpm (Fisher Scientific Centrifuge) for 5 min. The pelleted cells were additionally washed in 5 mL of HBSS-HEPES buffer (Hank's balanced salt solution containing 20 mM HEPES, Table 2.4) and pelleted by centrifugation at 3000 rpm (Fisher Scientific Centrifuge) for 5 minutes. The pelleted cells were then resuspended in 1 mL of HBSS-HEPES buffer. In a black, clear-bottomed, poly-D-lysine coated 96-well plate, 100 µL of the cell suspension (approximately 250,000 cells per well) was added per well and incubated at 37° C for 40 minutes while ligand dilutions (stimulation buffer) were prepared.

An increasing concentration of ligand (isoproterenol or carbachol in 10% dimethyl sulfoxide (DMSO)) was prepared in HBSS-HEPES buffer (stimulation buffer) according to the

optimal values in which to generate a dose-response curve. The range of ligand concentrations for each was 0-0.01 mM, except the carbachol stimulated assay using the SSQ or QSQ chimera with PTX added in which a range of 0-0.001 mM was used. Interestingly, studies have shown a synergistic relationship between β_2 AR and ascorbic acid²⁷. More specifically, ascorbic acid was found to enhance the receptors sensitivity and duration of action while the receptor was found to assist ascorbic acid's antioxidant activity by converting it to its reduced, useful form. Additionally, because isoproterenol is susceptible to oxidation^{28, 29}, ascorbic acid was added to the stimulation buffer at a final concentration of 1 mM. The competitive nonselective phosphodiesterase inhibitor 3-isobutyl-1-methylxanthine (IBMX) was added at a final concentration of 0.2 mM to inhibit the degradation of cAMP within the cell. After the addition of 50 μ L of stimulation buffer to each well containing an adherent monolayer of cells using a multichannel pipette (final volume in each well was 150 μ L), the absorbance of the plates was immediately measured at 535 nm and 612 nm every 13 s for 30 min using a microplate reader (GENios Pro, Tecan).

2.2.5 Data Analysis

Excel was used to baseline-normalize the time scale to disregard the first 26 s to account for mixing error (26 s set as 0 s). The difference between the first fluorescence data point and each data point thereafter until the 230th time point was calculated to attain the change in cAMP accumulation over time. This range was chosen as it reflected the linear portion of the initial increase in fluorescence. A curve was fit with nonlinear regression to generate the log dose-response relationship using GraphPad Prism 6. The data was then normalized to the maximum

observed response per data set using nonlinear regression to generate a log dose-percent response (cAMP accumulation) curve for comparison between chimera data.

3. Results

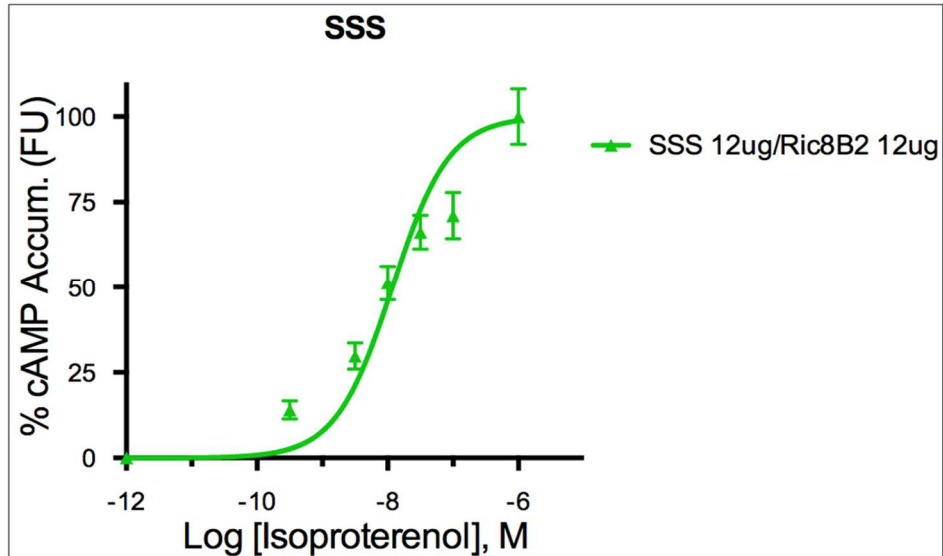


Figure 3.1: Analysis of wild type $G\alpha_s$ protein induced cAMP accumulation using the Pink Flamindo cAMP biosensor in Δ GNAS cells. cAMP accumulation is represented as percentage normalized to the maximum agonist-induced response individual in fluorescence units (FU). All assays were performed on an adherent monolayer (250,000 cells/well) of Δ GNAS cells (HEK293 cells lacking endogenous $G\alpha_s$ isoforms) in the presence of IBMX (0.2 mM) and ascorbic acid (1 mM). Absorbance was measured at 535 nm and 612 nm every 13 s for 30 min using a microplate reader (GENios Pro, Tecan). The dose-response curve represents the initial rate of increase (slope) in fluorescence units from 26-230 s. Cells were stimulated with a range of isoproterenol (β_2 AR agonist) and co-transfected with 12 μ g wild-type $G\alpha_s$ (SSS) and 12 μ g of the protein chaperone Ric-8B2. The data is represented by the means of four independent experiments \pm SEM in green.

To serve as an initial positive control displaying efficient receptor coupling and $G\alpha_s$ protein subunit activation, Δ GNAS cells containing a stably expressed cAMP sensor (Pink Flamindo) were co-transfected with the wild type $G\alpha_s$ protein subunit and the protein chaperone Ric-8B2 then stimulated with a range of isoproterenol in the presence of IBMX and ascorbic acid (Figure 3.1). Figure 3.1 shows a dose-response relationship characteristic of isoproterenol

stimulated β_2 AR which classically leads to cAMP production via adenylyl cyclase following the activation of $G\alpha_s$ protein subunits as a normalized percentage of cAMP accumulation. The EC_{50} was 10 nM, which is within the expected range of this system based on previous data.

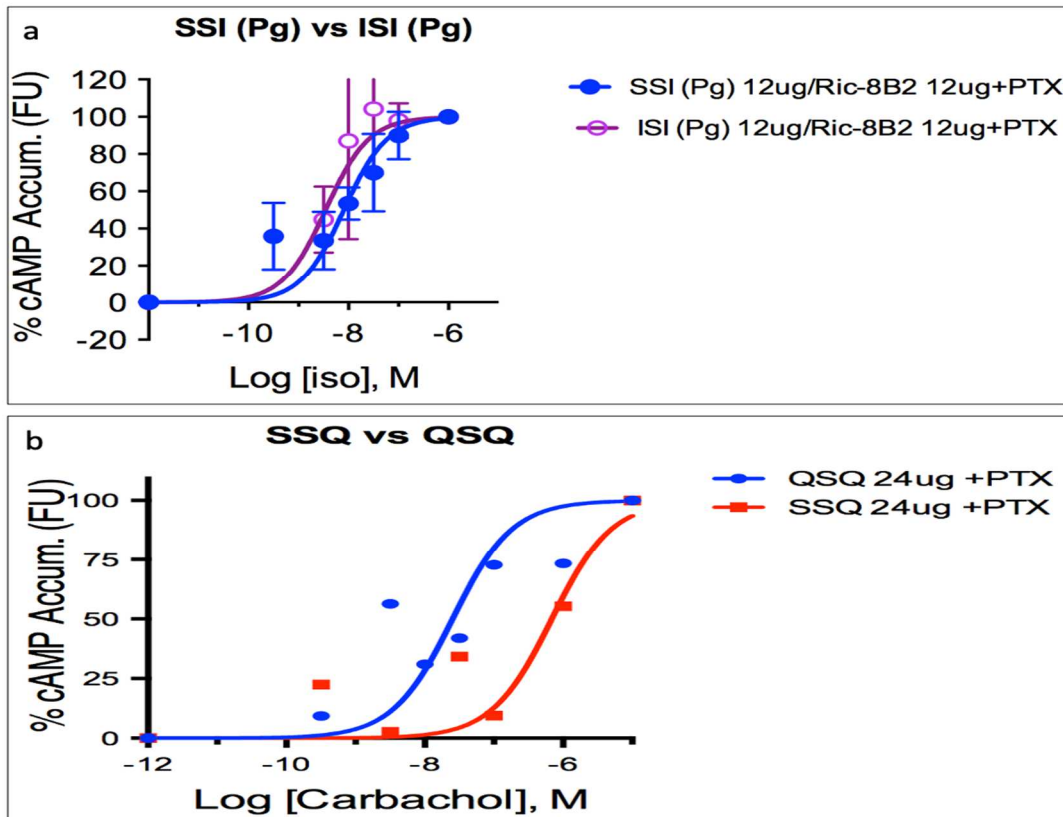


Figure 3.2: Analysis of $G\alpha_s$ -based chimera induced cAMP accumulation using the Pink Flamindo cAMP biosensor in Δ GNAS cells. cAMP accumulation is represented as percentage normalized to the maximum agonist-induced response individual to each chimeric $G\alpha_s$ protein in fluorescence units (FU). All assays were performed on an adherent monolayer (250,000 cells/well) of Δ GNAS cells (HEK293 cells lacking endogenous $G\alpha_s$ isoforms) in the presence of IBMX (0.2 mM) and ascorbic acid (1mM). Absorbance was measured at 535 nm and 612 nm every 13 s for 30 min using a microplate reader (GENios Pro, Tecan). The dose-response curves represent the initial rate of increase (slope) in cAMP from 26-230 seconds. **(a)** cAMP assay in which pertussis toxin (PTX) treated cells were stimulated with a range of isoproterenol (iso). Cells were co-transfected with 12 μ g of SSI (Pg)* in blue (n=5, error bars represent \pm SEM) ($G\alpha_s$ with the carboxy-terminus from $G\alpha_i$) or 12 μ g of ISI (Pg)* in purple (n=2, error bars represent \pm SEM) ($G\alpha_s$ with the amino- and carboxy-termini swapped with $G\alpha_i$) along with 12 μ g of the protein chaperone Ric-8B2. **(b)** cAMP assay in which PTX treated cells were stimulated with a range of carbachol in 10% DMSO (M_3 agonist). Cells were transfected with 24 μ g of SSQ in red (n=1, in duplicate) ($G\alpha_s$ with the carboxy-terminus from $G\alpha_q$) or 24 μ g of QSQ in blue (n=1, in duplicate) ($G\alpha_s$ with the amino- and carboxy-termini swapped with $G\alpha_q$) along with 12 μ g of the protein chaperone Ric-8B2. * (Pg) represents a C352G mutation to make the chimera insensitive to pertussis toxin.

To investigate the contributions of the amino- and carboxy-termini of $G\alpha$ protein subunits, a collection of chimeric $G\alpha_s$ -based protein subunits were created in which the amino- and carboxy-termini were systematically swapped with those of either $G\alpha_i$ or $G\alpha_q$ and transfected into Δ GNAS cells containing a stably expressed cAMP sensor (Pink Flamindo) that functioned as an indirect readout of receptor coupling specificity and $G\alpha$ protein subunit activation (Figure 3.2). As a first step toward understanding the contributions of the termini towards coupling and exchange, we studied the effects of isoproterenol on activation of endogenously expressed β_2 AR and measured its coupling efficiency to the $G\alpha$ chimeras. PTX was added to all assays to inhibit endogenous $G\alpha_i$ protein subunits to effectively isolate the effects the specific chimeric $G\alpha_s$ protein subunits have on cAMP production. In Figure 3.2a Δ GNAS cells were co-transfected with a $G\alpha_s$ -based chimera in which the C-term was replaced with that of a pertussis insensitive version of $G\alpha_i$ (SSI (Pg), blue) or $G\alpha_s$ -based double chimera in which the N- and C-termini were replaced with that of a pertussis insensitive version of $G\alpha_i$ (ISI (Pg), purple), and Ric-8B2. As illustrated, isoproterenol (iso) potently activated adenylyl cyclase activity (enhanced cAMP) through SSI ($EC_{50} \sim 8.1$ nM, $n=5$) and then the slightly more sensitive ISI ($EC_{50} \sim 3.5$ nM, $n=2$), albeit not statistically powered to be conclusive. The sensitivity of the chimeras to isoproterenol appears to display similar behavior to wild type- $G\alpha_s$ (SSS). We would have predicted that the native $G\alpha_s$ N-term on SSI should have displayed enhanced coupling of the $G\alpha_i$ C-term chimera over the $G\alpha_i$ N-term containing chimera (ISI). Clearly, further experimentation (repetitions) is required to determine whether the $G\alpha_s$ N-term couples better than $G\alpha_i$ N-term.

Similarly, in Figure 3.2b, PTX pre-treated Δ GNAS cells were transfected with a $G\alpha_s$ -based chimera in which the C-term was replaced with that of $G\alpha_q$ (SSQ, red) or $G\alpha_s$ -based double chimera in which the N- and C-term were replaced with that of $G\alpha_q$ (QSQ, Figure 3.2b, blue). The cells were stimulated with a range of carbachol concentrations (in 10% DMSO) and the EC_{50} was found to be 985 nM (n=1, in duplicate) for SSQ and 33 nM (n=1, in duplicate) for QSQ, which is less than the single replacement chimera (SSQ). In this case, we were targeting endogenously expressed M_3AChR . Altogether, based on the EC_{50} values at this point, these data suggest the amino-terminus plays an important role towards efficient downstream signaling.

Table 2.6: Summary of EC_{50} Values

Chimera (NBC name)	EC_{50} (nM)	Agonist Used	Receptor Targeted
SSS	10	Isoproterenol	β_2AR
SSI	8.1	Isoproterenol	β_2AR
ISI	3.5	Isoproterenol	β_2AR
SSQ	985	Carbachol	M_3AChR
QSQ	33	Carbachol	M_3AChR

4. Discussion

Multiple sources of evidence suggest that the N- and C-terminal ends of G protein α -subunits contribute toward receptor-G protein selectivity and to coupling efficiency. Early biochemical studies suggested that the $G\alpha$ C-term makes the key contribution toward receptor coupling thus toward receptor-G protein specificity. More recent structural evidence, however, have uncovered significantly larger surfaces on $G\alpha$ that contribute toward receptor binding and

G protein activation. These studies have shown that while GPCRs indeed have extensive interactions with the C-term of the G α subunit, the N-term has an equally important role interacting with the intracellular loops of GPCRs e.g., ICL2. This structural data is in good agreement with more recent biochemical and biophysical evidence which support the critical role of the G α N-term to receptor specificity but more importantly brings attention to a role relating to G protein activation through promoting nucleotide release.

While the role of the C-term is important and seems logical, when the promotion of GDP-release (nucleotide exchange) is considered in the context of other G proteins, such as the small molecular weight ras family, the logic weakens. The ras family incidentally displays a strong similarity to the nucleotide-binding domain (RHD) of G α subunits and do not rely on their C-term to promote nucleotide exchange. Instead, nucleotide exchange is promoted through disruption of the P-loop, which is the major site of interaction with the β -[PO₄]⁻ of GDP⁵⁶. As mentioned previously, the P-loop is linked to the N-term in G α subunits by the highly conserved β 1-strand. Therefore, in light of the mechanism involved in ras activation/nucleotide release, the structural evidence supporting the role of the N-term of G α with respect to nucleotide exchange seems reasonable.

Another example of the importance of regions outside of the C-term of G α involves the affinity of various forms of guanine nucleotides: GMP, GDP, and GTP. The initial arguments supported by early biochemical data in favor of the critical role of the C-term or α 5 helix were based on the fact that the loop between the β 6-strand and the α 5 helix (β 6- α 5 loop) contains residues that coordinate the purine ring of GDP and GTP. It appeared logical that perturbing the β 6- α 5 loop might affect the coordination of the purine ring and allow nucleotide release. However, the significance of the purine ring is hindered when GMP is considered. GMP contains

the same purine ring as GDP and GTP, but has 10^4 - 10^5 -fold lower affinity than GDP for $G\alpha$ subunits, just like ras-like G proteins¹¹. Moreover, the fundamental difference between GMP and GDP (monophosphate vs diphosphate) is the β -[PO₄] which happens to be the phosphate coordinated by the P-loop¹¹. Thus, it appears logical that the N-term must be intimately involved in nucleotide release through its connection to the P-loop. This reasoning is supported by recent structural data showing the N-term of $G\alpha$ interacting with ICL2 of GPCRs, regions which mutagenesis studies have strongly implicated in G protein coupling, which is consistent with the N-term's role in G protein activation. Therefore, with the support of recently published studies and our known preliminary data on the G protein chimeras, the shared contributions of both the N- and C-term in receptor-G protein coupling, G protein activation and toward receptor-G protein specificity were explored.

In our studies, we decided to use the core of $G\alpha_s$ to assemble the chimeras and measure the real-time cAMP accumulation using the Pink Flamindo biosensor because $G\alpha_s$ activates adenylyl cyclase through direct interaction with its Switch II domain, which is located well away from the N- and C-term and unrelated to nucleotide exchange⁵⁰. We also decided to take advantage of an HEK293-derived cell line in which the gene encoding $G\alpha_s$ (GNAS) has been disrupted. This Δ GNAS cell line displays low endogenous adenylyl cyclase activity under basal conditions and is insensitive to stimulation by Gs-coupled receptor activation¹⁵. Therefore, stimulation of β_2 AR with isoproterenol in Δ GNAS lines leads to decreases in cAMP accumulation through recruitment of the endogenous inhibitory G protein (Gi), which has also been found to couple to β_2 AR¹³. Additionally, to control for a potential coupling of β_2 AR to endogenous $G\alpha_i$, the cells were treated with pertussis toxin (PTX), which prevents $G\alpha_i$ from interacting with the receptor, as previously mentioned. Furthermore, we utilized point mutants of

G α chimeras containing the c-term of G α_i , where the residue that is normally ribosylated by PTX is mutated (C351G mutation). This allowed us to use PTX to exclude the contributions of endogenous G α_i signaling and focus only on the interaction, coupling, and activation of the PTX-insensitive G α_i C-term-containing chimeras.

In our study, we observed that overexpression of the G α_s -based single replacement chimeras with the carboxy-terminus of G α_i (SSI (Pg)) caused an increase in cAMP generation after isoproterenol stimulation through the β_2 AR, which suggests that the C-term of G α_i is fully capable of coupling and activation via β_2 AR. Unfortunately, time limitations have disrupted our ability to establish a complete data set on β_2 AR coupling to SSS, SSI and ISI. Our preliminary data suggests that the G α_i N-term in the ISI chimeras displays slightly higher affinity for isoproterenol than the SSI chimera, although our data are not statistically powered enough to determine whether these differences are significant.

The same relationship was seen with the G α_s -based C-term replacement with that of G α_q (SSQ). Application of carbachol and stimulation of endogenous M $_3$ AChR led to activation of the SSQ chimera (i.e. gained a G α_q coupling capacity) and stimulation of adenylyl cyclase. The M $_3$ AChR is a classic Gq-coupled receptor that regulates calcium signaling via IP $_3$ generation. Since we utilized the Δ GNAS cell lines, it is safe to assume that cyclase responses are a direct result of the G α_s -based chimera coupling to the M $_3$ AChR when endowed with the G α_q C-term. These findings are in good agreement with previous data from Conklin et al. (1996) which showed that when the carboxy-termini are swapped between G α_q and G α_z subunits, receptors will activate chimera appropriate to which carboxy-termini is present and cognate to M $_3$ AChR⁴⁷.

More notably, when the $G\alpha_q$ N- and C-term containing double chimera QSQ is considered, a 30-fold difference in EC50 was observed when compared to that of SSQ (33 nM vs 985 nM, respectively). This difference suggests that the N-term greatly contributes to the M_3AChR selection process and leads to more efficient G protein activation, giving the double chimera close to Gq-like qualities. This finding is in good agreement with previously published data suggesting that Gq-coupled receptors, such as M_3AChR , use the N-term of $G\alpha_q$ as a selectivity filter ⁴⁸. Additionally, Jelinick et al. (2021) found that when both termini were replaced on $G\alpha_o$ with that of $G\alpha_q$, the chimera gained qualities comparable to wild type Gq results (receptor-G protein complex stabilities and G protein activation results) when coupled to M_3AChR ⁴⁹. While conclusions made about our data make sense based on the number of repetitions completed, a conclusive assignment of significance can only be attained after more repetitions are compiled. Ultimately, previous literature suggest that the C-term is not the sole contributor related to a receptor's selectivity process but implicates the N-term as a synergistic partner.

5. Conclusions

In conclusion, we engineered a set of $G\alpha_s$ -based chimeras by swapping the N- and C-termini from that of either $G\alpha_i$ or $G\alpha_q$. The goal of which was to uncover the contributions of the N- and C-termini towards efficient downstream signaling and receptor specificity by using cAMP accumulation as an indirect means of measurement. It was hypothesized that both the N- and the C-term contribute to efficient second messenger generation. While the results of this study are inconclusive based on the number of experimental repetitions completed and the lack of statistical analysis, the results compiled from an extended literature review support the notion

that both the N- and C-term play a role in receptor-G protein selectivity and efficient G protein activation. More specifically, it appears that the N-terminus and all 22 amino acids from the C-term majorly contribute to coupling specificity. Altogether, these results and literature reviewed in this study potentially detail important insights regarding GPCR-G protein selectivity and identify motifs within the $G\alpha$ subunit that appear to initiate efficient downstream signaling. Additionally, we hope that exploring the intricacies of GPCR-G protein selectivity provides insight into on-target, yet signal-biased, drug side effects. By gaining a deeper understanding of how ligands, such as salmeterol, can stabilize coupling to one G protein isoform over another isoform in the context of the G protein's N- and C-term composition, we may uncover the underlying factors that dictate a universal mechanism of receptor-G protein selection. Attaining this knowledge may aid in the design and development of safer therapeutics.

5.1 Future Studies

Due to time limitations, we could not collect enough technical and biological repetitions on the agonist-stimulated activation of the chimeras. More repetitions will need to be completed in order to determine the EC_{50} values in at least three independent experiments. The EC_{50} values from agonist stimulated, cognate receptor-G protein pairs could then be compared statistically to each chimera containing the respective N- and C-termini from the cognate pair using a t-test, e.g., the EC_{50} value from carbachol stimulation of the M_2AChR coupling to $G\alpha_i$ compared to the EC_{50} 's of ISI and SSI chimera also coupling to the M_2AChR after carbachol stimulation. Additionally, there are several controls that are required, including being able to exclude the possibility that the M_3AChR is activating adenylyl cyclase independent of the transfected chimeras. This could be done by giving $\Delta GNAS$ cells carbachol and generating a dose-response

curve in the absence of any chimera. Another control would be to co-transfect Ric-8B2 with each chimera and repeat the wild-type $G\alpha_s$ measurements with PTX. Also, it would be wise to assess whether the chimeric G proteins were expressed at similar levels to each other and to the wild type versions. Fortunately, we froze and stored 100 μ L aliquots of cells from each transfection and each assay, which allows us to assess expression levels by western blotting analysis in the future. It is also possible to stably express a chimera with a tetracycline-regulated promoter in order to attain equal expression levels of the chimeras, should transient expression be variable. Similarly, while beyond the scope of this study, we may attempt to obtain cryoEM structures of the receptor-bound chimeras to examine how matched, or cognate termini, interact with a receptor in comparison to non-cognate termini. Finally, this chimeric strategy could also be extended to other G protein isoforms to see if the same relationships can be observed which could lead to the discovery of a universal mechanism. We also plan to expand the screen of coupling efficiency of the chimeras beyond the β_2 AR and M_3 AChR. Our next candidate class of receptors are the G_i -coupled forms, most notably the mu-opioid (MOR), dopamine D2 (DRD2) and M_2 muscarinic receptors (M_2 AChR). The future directions listed here should guide us towards a predictable mechanism of ligand-receptor-G protein trio interactions.

References:

1. Conklin, B. R., & Bourne, H. R. (1993). Structural elements of G α subunits that interact with G $\beta\gamma$, receptors, and effectors. *Cell*, 73(4), 631–641. doi:10.1016/0092-8674(93)90245-l
2. Wess, J. (1997). G-protein-coupled receptors: molecular mechanisms involved in receptor activation and selectivity of G-protein recognition. *The FASEB Journal*, 11(5), 346–354. doi:10.1096/fasebj.11.5.9141501
3. Strader, C. D., Fong, T. M., Tota, M. R., Underwood, D., & Dixon, R. A. (1994). Structure and function of G protein-coupled receptors. *Annual review of biochemistry*, 63(1), 101-132.
4. Rens-Domiano, S., & Hamm, H. E. (1995). Structural and functional relationships of heterotrimeric G-proteins. *The FASEB Journal*, 9(11), 1059–1066. doi:10.1096/fasebj.9.11.7649405
5. Conklin, B. R., Farfel, Z., Lustig, K. D., Julius, D., & Bourne, H. R. (1993). Substitution of three amino acids switches receptor specificity of G α_q to that of G α_i . *Nature*, 363(6426), 274–276. doi:10.1038/363274a0
6. Kostenis, E., Conklin, B. R., & Wess, J. (1997). Molecular Basis of Receptor/G Protein Coupling Selectivity Studied by Coexpression of Wild Type and Mutant m2 Muscarinic Receptors with Mutant G α_q Subunits†. *Biochemistry*, 36(6), 1487–1495. doi:10.1021/bi962554d
7. Flock, T., Hauser, A. S., Lund, N., Gloriam, D. E., Balaji, S., & Babu, M. M. (2017). Selectivity determinants of GPCR–G-protein binding. *Nature*, 545(7654), 317–322. doi:10.1038/nature22070
8. Sandhu, M., Touma, A. M., Dysthe, M., Sadler, F., Sivaramakrishnan, S., & Vaidehi, N. (2019). Conformational plasticity of the intracellular cavity of GPCR–G-protein complexes leads to G-protein promiscuity and selectivity. *Proceedings of the National Academy of Sciences*, 201820944. doi:10.1073/pnas.1820944116
9. Semack, A., Sandhu, M., Malik, R. U., Vaidehi, N., & Sivaramakrishnan, S. (2016). Structural Elements in the Gas and G α_q C Termini That Mediate Selective G Protein-coupled Receptor (GPCR) Signaling. *Journal of Biological Chemistry*, 291(34), 17929–17940. doi:10.1074/jbc.m116.735720
10. Bockaert, J., & Pin, J. P. (1999). Molecular tinkering of G protein-coupled receptors: an evolutionary success. *The EMBO journal*, 18(7), 1723-1729.
11. Mahoney, J. P., & Sunahara, R. K. (2016). Mechanistic insights into GPCR–G protein interactions. *Current Opinion in Structural Biology*, 41, 247–254. doi:10.1016/j.sbi.2016.11.005
12. Nestler EJ, Duman RS. Heterotrimeric G Proteins. In: Siegel GJ, Agranoff BW, Albers RW, et al., editors. *Basic Neurochemistry: Molecular, Cellular and Medical Aspects*. 6th edition.

Philadelphia: Lippincott-Raven; 1999. Available from:
<https://www.ncbi.nlm.nih.gov/books/NBK28116/>

13. Pierce, K. L., Premont, R. T., & Lefkowitz, R. J. (2002). Seven-transmembrane receptors. *Nature Reviews Molecular Cell Biology*, 3(9), 639–650. doi:10.1038/nrm908
14. Essayan, D. M. (2001). Cyclic nucleotide phosphodiesterases. *Journal of Allergy and Clinical Immunology*, 108(5), 671–680. doi:10.1067/mai.2001.119555
15. Hesley, J., Daijo, J., Ferguson, A.T. (2002). Stable, Sensitive, Fluorescence-Based Method for Detecting cAMP. *BioTechniques*, 33(3), 691–694. doi:10.2144/02333dd05
16. Apter, A. J., Reisine, S. T., Willard, A., Clive, J., Wells, M., Metersky, M., McNally, D., ZuWallack, R. L. (1996). The effect of inhaled albuterol in moderate to severe asthma. *Journal of Allergy and Clinical Immunology*, 98(2), 295–301. doi:10.1016/s0091-6749(96)70153-7
17. Lee, Y., Basith, S., & Choi, S. (2017). Recent Advances in Structure-Based Drug Design Targeting Class A G Protein-Coupled Receptors Utilizing Crystal Structures and Computational Simulations. *Journal of Medicinal Chemistry*, 61(1), 1–46. doi:10.1021/acs.jmedchem.6b01453
18. Masureel, M., Zou, Y., Picard, L.-P., van der Westhuizen, E., Mahoney, J. P., Rodrigues, J. P. G. L. M., Mildorf, T. J., Dror, R. O., Shaw, D. E., Bouvier, M., Pardon, E., Steyaert, J., Sunahara, R. K., Weis, W. I., Zhang, C., Kobilka, B. K. (2018). Structural insights into binding specificity, efficacy and bias of a β 2AR partial agonist. *Nature Chemical Biology*, 14(11), 1059–1066. doi:10.1038/s41589-018-0145-x
19. Melien, Ø. (2007). Heterotrimeric G Proteins and Disease. *Target Discovery and Validation Reviews and Protocols*, 119–144. doi:10.1385/1-59745-208-4:119
20. Sprang, S. R. (1997). G PROTEIN MECHANISMS: Insights from Structural Analysis. *Annual Review of Biochemistry*, 66(1), 639–678. doi:10.1146/annurev.biochem.66.1.639
21. Moss, J., & Vaughan, M. (1979). *Activation of Adenylate Cyclase by Cholera toxin. Annual Review of Biochemistry*, 48(1), 581–600. doi:10.1146/annurev.bi.48.070179.003053
22. Mathiesen, J. M., Vedel, L., & Bräuner-Osborne, H. (2013). cAMP Biosensors Applied in Molecular Pharmacological Studies of G Protein-Coupled Receptors. *G Protein Coupled Receptors - Modeling, Activation, Interactions and Virtual Screening*, 191–207. doi:10.1016/b978-0-12-407865-9.00011-x
23. Simon, M., Strathmann, M., & Gautam, N. (1991). *Diversity of G proteins in signal transduction. Science*, 252(5007), 802–808. doi:10.1126/science.1902986
24. Mangmool, S., & Kurose, H. (2011). *Gi/o Protein-Dependent and -Independent Actions of Pertussis Toxin (PTX). Toxins*, 3(7), 884–899. doi:10.3390/toxins3070884

25. Harada, K., Ito, M., Wang, X., Tanaka, M., Wongso, D., Konno, A., Hirai, H., Hirase, H., Tsuboi, T., Kitaguchi, T. (2017). Red fluorescent protein-based cAMP indicator applicable to optogenetics and in vivo imaging. *Scientific Reports*, 7(1).doi:10.1038/s41598-017-07820-6
26. Vasudevan, N. T. (2017). cAMP assays in GPCR drug discovery. *G Protein-Coupled Receptors Part A*, 51–57. doi:10.1016/bs.mcb.2017.07.014
27. Dillon, P. F., Root-Bernstein, R., Robinson, N. E., Abraham, W. M., Berney, C. (2010). “Receptor-Mediated Enhancement of Beta Adrenergic Drug Activity by Ascorbate in Vitro and in Vivo.” *PLoS ONE*, vol. 5, no. 12, 2010, <https://doi.org/10.1371/journal.pone.0015130>.
28. Nayak, A. S., Cutie, A. J., Jochsberger, T., Kay, A. I. (2008). “The Effect of Various Additives on the Stability of Isoproterenol Hydrochloride Solutions.” *Drug Development and Industrial Pharmacy*, vol. 12, no. 4, 1986, pp. 589–601., <https://doi.org/10.3109/03639048609048031>.
29. Van der Westhuizen, E. T., Breton, B., Bouvier, M. (2013). “Quantification of Ligand Bias for Clinically Relevant B2-Adrenergic Receptor Ligands: Implications for Drug Taxonomy.” *Molecular Pharmacology*, vol. 85, no. 3, 2013, pp. 492–509., <https://doi.org/10.1124/mol.113.088880>.
30. Birnbaumer, Lutz. (2007). “Expansion of Signal Transduction by G Proteins.” *Biochimica Et Biophysica Acta (BBA) - Biomembranes*, vol. 1768, no. 4, 2007, pp. 772–793., <https://doi.org/10.1016/j.bbamem.2006.12.002>.
31. Rasmussen, S.G., DeVree, B. T., Zou, Y., Kruse, A. C., Chung, K. Y., Kobilka, T. S., Thian, F. S., Chae, P. S., Pardon, E., Calinski, D., Mathiesen, J. M., Shah, S. T. A., Lyons, J. A., Caffrey, M., Gellman, S. H., Steyaert, J., Skiniotis, G., Weis, W. I., Sunahara, R. K., Kobilka, B. K. (2011). “Crystal Structure of the β_2 Adrenergic Receptor–GS Protein Complex.” *Nature*, vol. 477, no. 7366, 2011, pp. 549–555., <https://doi.org/10.1038/nature10361>.
32. Johnson, E. N., & Druey, K. M. (2002). Heterotrimeric G protein signaling: Role in asthma and allergic inflammation. *Journal of Allergy and Clinical Immunology*, 109(4), 592–602. doi:10.1067/mai.2002.122636
33. Goricanec, D., Stehle, R., Egloff, P., Grigoriu, S., Plückthun, A., Wagner, G., Hagn, F. (2016). “Conformational Dynamics of a G-Protein α Subunit Is Tightly Regulated by Nucleotide Binding.” *Proceedings of the National Academy of Sciences*, vol. 113, no. 26, 2016, <https://doi.org/10.1073/pnas.1604125113>.
34. Xiuyan, M., Hu, Y., Batebi, H., Heng, J., Xu, J., Liu, X., Niu, X., Li, H., Hildebrand, P. W., Jin, C., Kobilka, B. K. (2020). “Analysis of β_2 ar-GSAND β_2 ar-Gicomplex Formation by NMR Spectroscopy.” *Proceedings of the National Academy of Sciences*, vol. 117, no. 37, 2020, pp. 23096–23105., <https://doi.org/10.1073/pnas.2009786117>.

35. Du, Y., Duc, N. M., Rasmussen, S. G. F., Hilger, D., Kubiak, X., Wang, L., Bohon, J., Kim, H. R., Wegrecki, M., Asuru, A., Jeong, K.M., Lee, J., Chance, M. R., Lodowski, D. T., Kobilka, B. K., Chung, K. Y. (2019). "Assembly of a GPCR-G Protein Complex." *Cell*, vol. 177, no. 5, 2019, <https://doi.org/10.1016/j.cell.2019.04.022>.
36. Klarenbeek, J., Goedhart, J., van Batenburg, A., Groenewald, D., & Jalink, K. (2015). Fourth-Generation Epac-Based FRET Sensors for cAMP Feature Exceptional Brightness, Photostability and Dynamic Range: Characterization of Dedicated Sensors for FLIM, for Ratiometry and with High Affinity. *PLOS ONE*, 10(4), e0122513. doi:10.1371/journal.pone.0122513
37. Oldham, W. M., & Hamm, H. E. (2008). Heterotrimeric G protein activation by G-protein-coupled receptors. *Nature Reviews Molecular Cell Biology*, 9(1), 60–71. doi:10.1038/nrm2299
38. Tan, L., Yan, W., McCorvy, J. D., & Cheng, J. (2018). Biased Ligands of G Protein-Coupled Receptors (GPCRs): Structure–Functional Selectivity Relationships (SFSRs) and Therapeutic Potential. *Journal of Medicinal Chemistry*. doi:10.1021/acs.jmedchem.8b00435
39. Dascal, N. (2001). Ion-channel regulation by G proteins. *Trends in Endocrinology and Metabolism*, 12(9), 391–398. doi:10.1016/s1043-2760(01)00475-1
40. Kamato, D., Thach, L., Bernard, R., Chan, V., Zheng, W., Kaur, H., Brimble, M., Osman, N., Little, P. J. (2015). Structure, Function, Pharmacology, and Therapeutic Potential of the G Protein, G $\hat{1}\pm/q,11$. *Frontiers in Cardiovascular Medicine*, 2. doi:10.3389/fcvm.2015.00014
41. Weinstein, L. S., Yu, S., Warner, D. R., & Liu, J. (2001). Endocrine Manifestations of Stimulatory G Protein α -Subunit Mutations and the Role of Genomic Imprinting. *Endocrine Reviews*, 22(5), 675–705. doi:10.1210/edrv.22.5.0439
42. Seven, A. B., Hilger, D., Papasergi-Scott, M. M., Zhang, L., Qu, Q., Kobilka, B. K., Tall G. G., Skiniotis, G., Skiniotis, G. (2020). Structures of G α Proteins in Complex with Their Chaperone Reveal Quality Control Mechanisms. *Cell Reports*. doi:10.1016/j.celrep.2020.02.08
43. Papasergi, M. M., Patel, B. R., & Tall, G. G. (2014). The G Protein Chaperone Ric-8 as a Potential Therapeutic Target. *Molecular Pharmacology*, 87(1), 52–63. doi:10.1124/mol.114.094664
44. Carpenter, B., Nehmé, R., Warne, T., Leslie, A. G. W., & Tate, C. G. (2016). Structure of the adenosine A2A receptor bound to an engineered G protein. *Nature*, 536(7614), 104–107. doi:10.1038/nature18966
45. Zhao, P., Metcalf, M., Bunnett, N. W. (2014). Biased Signaling of Protease-Activated Receptors. *Frontiers in Endocrinology*, 5(), –. doi:10.3389/fendo.2014.00067

46. Conklin, B. R., Farfel, Z., Lustig, K. D., Julius, D., & Bourne, H. R. (1993). Substitution of three amino acids switches receptor specificity of Gq α to that of Gi α . *Nature*, 363(6426), 274–276. doi:10.1038/363274a0
47. Conklin, B. R., Herzmark, P., Ishida, S., Voyno-Yasenetskaya, T. A., Sun, Y., Farfel, Z., & Bourne, H. R. (1996). Carboxyl-terminal mutations of Gq α and Gs α that alter the fidelity of receptor activation. *Molecular pharmacology*, 50(4), 885–890.
48. Kostenis, E., Degtyarev, M. Y., Conklin, B. R., & Wess, J. (1997). The N-terminal Extension of Gq α s Critical for Constraining the Selectivity of Receptor Coupling. *Journal of Biological Chemistry*, 272(31), 19107–19110. doi:10.1074/jbc.272.31.19107
49. Jelinek, V., Mösslein, N., Bünemann, M. (2021). “Structures in G Proteins Important for Subtype Selective Receptor Binding and Subsequent Activation.” *Communications Biology*, vol. 4, no. 1, 2021, <https://doi.org/10.1038/s42003-021-02143-9>.
50. Sadana, R., Dessauer, C. W. (2009). Physiological Roles for G Protein-Regulated Adenylyl Cyclase Isoforms: Insights from Knockout and Overexpression Studies. *Neurosignals*, 17(1), 5–22. doi:10.1159/000166277
51. Sriram, K., Insel, P. A. (2018). GPCRs as targets for approved drugs: How many targets and how many drugs?. *Molecular Pharmacology*, mol.117.111062–. doi:10.1124/mol.117.111062
52. Fan, G., Jiang, Y., Lu, Z., Martin, D. W., Kelly, D. J., Zuckerman, J. M., Ballou, L. M., Cohen, I. S., Lin, R. Z. (2005). A Transgenic Mouse Model of Heart Failure Using Inducible Gq. *Journal of Biological Chemistry*, 280(48), 40337–40346. doi:10.1074/jbc.M506810200
53. Zhou, X. E., Melcher, K., Xu, H. E. (2018). Structural biology of G protein-coupled receptor signaling complexes. *Protein Science*. 28(3):487-50. doi:10.1002/pro.3526
54. Zhang, D., Zhao, Q., Wu, B. (2015). Structural Studies of G Protein-Coupled Receptors. *Molecules and Cells*, 38(10), 836–842. doi:10.14348/molcells.2015.0263
55. Herrmann, R.; Heck, M.; Henklein, P.; Henklein, P.; Kleuss, C.; Hofmann, K. P.; Ernst, O. P. (2004). Sequence of Interactions in Receptor-G Protein Coupling. *Journal of Biological Chemistry*, 279(23), 24283–24290. doi:10.1074/jbc.M311166200
56. Bos, J. L., Rehmann, H., Wittinghofer, A. (2007). GEFs and GAPs: Critical Elements in the Control of Small G Proteins. *129(5)*, 0–877. doi:10.1016/j.cell.2007.05.018
57. Verstraeten, N., Fauvart, M., Versees, W., Michiels, J. (2011). The Universally Conserved Prokaryotic GTPases. *Microbiology and Molecular Biology Reviews*, 75(3), 507–542. doi:10.1128/MMBR.00009-11

58. Osawa, S., Dhanasekaran, N., Woon, C. W., Johnson, G. L. (1990). *Gai- α s* chimeras define the function of α chain domains in control of G protein activation and $\beta\gamma$ subunit complex interactions. 63(4), 697–706. doi:10.1016/0092-8674(90)90136-3
59. Russell, M., Johnson, G. L. (1993) G protein amino-terminal α i2/ α s chimeras reveal amino acids important in regulating α s activity. *Mol Pharmacol.* 1993 Aug;44(2):255-63. PMID: 8394989.
60. Chen, X. P., Yang, W., Fan, Y., Luo, J. S., Hong, K., Wang, Z., Yan, J. F., Chen, X., Lu, J. X., Benovic, J. L., Zhou, N. M. (2010). Structural determinants in the second intracellular loop of the human cannabinoid CB1 receptor mediate selective coupling to Gs and Gi. 161(8), 1817–1834. doi:10.1111/j.1476-5381.2010.01006.x